Analysis and design of rhythmic neuromorphic networks through dominance and bifurcations

Omar Juarez-Alvarez, Alessio Franci

***Abstract*— The control of oscillator networks capable of exhibiting complex rhythmic behaviors is a fundamental engineering problem motivated by the analysis and design of a variety of rhythmic biological and artificial systems. This work aims at introducing new theoretical tools, grounded in dominance analysis and bifurcation theory, to analyze and design biological and bio-inspired rhythmic networks. We derive constructive conditions under which the spectral properties of the network adjacency matrix fully and explicitly determine both the emergence of a network rhythm and its detailed profile (oscillator amplitudes and phases). The derived conditions can be used for analysis, prediction, and control of the rhythmic behavior of an existing network or for the design of a rhythmic network with a desired rhythmic behavior. The modeling framework under which we develop our theory is motivated by neuromorphic engineering, which makes our approach compatible with both the architecture of rhythmic biological networks and with the technological constraints needed to design bio-inspired rhythmic networks in compact and energy-efficient neuromorphic electronics.**

***Index Terms*— Bifurcation theory, Central pattern generators, Network oscillations, Neuromorphic engineering, Rhythm control.**

I. Introduction

NETWORK rhythms are omnipresent in biology. Virtually all the basic biological functions we use to survive, like breathing, moving, swallowing, chewing, pumping blood, producing sounds, and alternating between sleep and wakefulness are rhythmic and to be functional they require the generation of well-coordinated rhythmic signals. Single-celled beings like bacteria use similar rhythmic signals to move, duplicate, consume nutrients, and produce the chemical signals that allow them to interact with other individuals. Many machines we design also need the generation of well-coordinated rhythmic signals, for instance, for the coordination of robotic arms employed in repeated pick-and-place tasks, or for any kind of moving robot using walking, crawling, or swimming as a way of locomotion. In both biological and artificial systems, the rhythmic signal is distributed across a network of nodes (different robotic manipulators, different legs, muscles, etc.) and the rhythms of different nodes must be coordinated so that the resulting network rhythm can accomplish a desired function, like picking and placing pieces in a well determined temporal order to build an artifact or swinging different extremities at different times to generate locomotion.

Biological rhythm-generating networks are particularly well studied and characterized in groups of neurons known as central pattern generators (CPGs) [1]–[4]. The rhythmic behavior of a CPG, described by the amplitudes and phases with which the electrical activity of each neuron in the CPG oscillates, determines its functional effects for the organism. For instance, a CPG in the horse motor system can produce a rhythm that successively contracts leg muscles to generate a trot gait but, as needed or as commanded, can change its rhythm to generate a walk gait [5]; a CPG in the crab digestive system can produce a rhythm to generate a motor behavior analogous to chewing but, depending on environmental and internal conditions, can change its rhythm to induce a motor behavior analogous to swallowing [2].

Biological CPGs need to be both modulable (to generate disparate rhythms) and robust (to cope with the variability and noise of biological components). It is well known that modulable and robust rhythms require positive and negative feedback in well-separated timescales [6], [7]. Neuromorphic engineering aims at implementing biological neuron functions (including CPGs) into compact and energy-efficient electronic circuits, and is a promising technology for low-power autonomous agent and edge applications [8]. Like their biological counterparts, neuromorphic engineering designs also rely on positive and negative feedback loops in well-separated timescales to achieve circuits that are both modulable and robust to electronic microcomponent mismatch and noise [9].

In robotics, the use of CPGs for generating coordinated gait signals has a long history (see, e.g., [10] and references therein). Similar strategies have also found applications in rehabilitation robotics [11]. Motivated by this applications, some efforts have been made to develop theoretical tools to design oscillator networks capable of generating desired rhythmic behaviors. However, to the best of our knowledge, none of the existing approaches is compatible with neuromorphic engineering applications for two main reasons: the used oscillator model is not compatible with neuromorphic hardware [12]–[14] and/or the rhythmic signals must be

This work was supported by the Belgian Government through the FPS Policy and Support (BOSA) grant NEMODEI.

Omar Juarez-Alvarez is with the Department of Mathematics, Universidad Nacional Autónoma de México, Ciudad de México, México (e-mail: pat_jualv@ciencias.unam.mx).

Alessio Franci is with the Montefiore Institute, University of Liege, Liege, Belgium, with the Department of Mathematics, Universidad Nacional Autónoma de México, Ciudad de México, México, and with the WEL Research Institute, Wavre, Belgium (e-mail: alessio.franci83@gmail.com).

endogenously generated and provided to the CPG [11].

In this paper we introduce novel theoretical tools to analyze and design the rhythmic behavior for neuromorphic oscillator networks. Our approach is constructive because the expressions we derive fully characterize the network rhythm and can easily be verified (for analysis) or imposed (for design) by studying (for analysis) or manipulating (for design) the network adjacency matrix. The slow-fast nature of neuromorphic oscillators is key to ensure that the spectral properties of the adjacency matrix determine the geometry of the low-dimensional dominant dynamics along which the network rhythm emerges through a Hopf bifurcation.

The paper is organized as follows. Notation and mathematical preliminaries are introduced in Section II. The slow-fast neuromorphic oscillator model is introduced in Section III. Section IV formalizes concepts to describe network rhythms and uses them to provide insight into the key objectives, ideas, and results of the paper. Section V formulates and discusses the meaning of the main "dominance" assumption. Section VI presents results characterizing the spectral properties of the network Jacobian in terms of the network adjacency matrix. Section VII builds on Section VI to characterize the leading eigenstructure of the model Jacobian and thus the network dominant dynamics. Section VIII presents the main results on constructive control of network rhythms. Section IX applies the results to the design of network rhythms. Conclusions and future directions are discussed in Section X. The most technical proofs are not included in the main text and can be found in Appendix I.

II. Mathematical preliminaries

A. Notation and basic definitions

Real N-dimensional vectors are denoted in bold $\boldsymbol{x}, \boldsymbol{v}, \boldsymbol{\zeta}, \ldots$, and are defined entry-wise as $\boldsymbol{x} = (x_1, x_2, \ldots, x_N) \in \mathbb{R}^N$. $\mathbf{0}_N = (0, \ldots, 0) \in \mathbb{R}^N$ denotes the zero vector, $\mathbf{1}_N = (1, \ldots, 1) \in \mathbb{R}^N$ the all-ones vector, and $\boldsymbol{e}_j = (\delta_{jk})_{k=1}^N \in \mathbb{R}^N$ canonical vectors, where δ_{jk} is the Kronecker delta. Complex numbers are either expressed in Cartesian form, $z = a + ib$, with $a \in \mathbb{R}$, $b \in \mathbb{R}$, or in polar form, $z = \rho e^{i\theta}$, for $\rho \geqslant 0$ and $\theta \in \mathbb{S}^1$, where $\mathbb{S}^1 := \mathbb{R} \bmod 2\pi$. The conjugation of a complex number $z = a+ib$ is $\overline{z} = a-ib$ and its modulus is $|z| = \sqrt{z\overline{z}}$. Complex vectors $\boldsymbol{z} \in \mathbb{C}^N$ are represented as $\boldsymbol{z} = \boldsymbol{a} + i\boldsymbol{b}$, where $\boldsymbol{a}, \boldsymbol{b} \in \mathbb{R}^N$ are the vector's real and imaginary parts, respectively. The conjugate of a complex vector, $\bar{\boldsymbol{z}} = \boldsymbol{a} - i\boldsymbol{b}$, is computed entry-wise. A complex vector $\boldsymbol{z} \in \mathbb{C}^N$ is said to be *modulus-homogeneous* if there exists $\kappa \geqslant 0$ such that $|\boldsymbol{z}_j| = \kappa$, for all $j \in \{1, \ldots, N\}$. The entry-wise Hadamard product of two complex vectors $\boldsymbol{z}$ and $\boldsymbol{y}$ is denoted by $\boldsymbol{z} \odot \boldsymbol{y} \in \mathbb{C}^N$ and defined entry-wise by $(\boldsymbol{z} \odot \boldsymbol{y})_i = z_i y_i$. We define two inner products: the matricial inner product $\boldsymbol{v}^t\boldsymbol{w}$, for real vectors, and the complex inner product $\langle \boldsymbol{v}, \boldsymbol{w} \rangle = \overline{\boldsymbol{v}}^t \boldsymbol{w}$, for complex vectors. Two indexed sets $U = \{\boldsymbol{u}_j \in \mathbb{C}^N : j \in \{1, \ldots, k\}\}$ and $V = \{\boldsymbol{v}_j \in \mathbb{C}^N : j \in \{1, \ldots, k\}\}$ form a *biorthogonal system* if for every $n \in \{1, \ldots, k\}$ and $m \in \{1, \ldots, k\}$ it holds that $\langle \boldsymbol{u}_n, \boldsymbol{v}_m \rangle = \delta_{nm}$.

A smooth function $S : \mathbb{R} \to \mathbb{R}$ is said to be a *locally odd sigmoid* if its satisfies (a) $S(0) = 0$, (b) $\forall\, x \in \mathbb{R} : S'(x) > 0$, and (c) $\operatorname{argmax} S'(x) = 0$. If S is at least three times differentiable, then condition (c) implies $S''(0) = 0$ and $S'''(0) \leqslant 0$. In the sequel we assume that $S'(0) = 1$ and $S'''(0) < 0$. For simulating purposes we consider $S = \tanh$. Given a parameterized vector field $\boldsymbol{f}(\boldsymbol{x}; p)$ in $\mathbb{R}^n$ which is k times differentiable, and an ordered set $\gamma = \{\boldsymbol{v}_1, \ldots, \boldsymbol{v}_k\} \subseteq \mathbb{R}^n$, the k-th order directional derivative of $\boldsymbol{f}$ along γ computed at $(\boldsymbol{x}, p)$ is defined as

$$(\mathrm{d}^k \boldsymbol{f})_{\boldsymbol{x},p}(\boldsymbol{v}_1, \ldots, \boldsymbol{v}_k) := \frac{\partial}{\partial t_1} \cdots \frac{\partial}{\partial t_k} \boldsymbol{f}\left(\boldsymbol{x} + \sum_{i=1}^k t_i \boldsymbol{v}_i; p\right)$$
$$= \sum \frac{\partial^k \boldsymbol{f}}{\partial x_{i_1} \ldots \partial x_{i_k}} (\boldsymbol{x}; p)(\boldsymbol{v}_1)_{i_1} \ldots (\boldsymbol{v}_k)_{i_k},$$

where the last sum is over all the k-th order partial derivatives of f.

We denote the set of $N \times N$ real and complex square matrices as $\mathbb{R}^{N\times N}$ and $\mathbb{C}^{N\times N}$, respectively. We denote the transpose of matrix A as A^t. Any N-tuple $\boldsymbol{x}$ is considered as a $N \times 1$ column matrix, while its transpose $\boldsymbol{x}^t$ is considered to be a $1 \times N$ row matrix. The zero matrix is denoted by $O_N = (0)_{ij} \in \mathbb{R}^{N\times N}$, and the identity matrix by $I_N = (\delta_{ij}) \in \mathbb{R}^{N\times N}$. A matrix $A = (a_{ij})$ is said to be positive (non-negative) if all of its entries a_{ij} are positive (non-negative) for every i, j. We similarly define positive and non-negative vectors. Given a set of complex numbers $\{z_1, \ldots, z_N\}$ we denote $D = \operatorname{diag}(z_1, \ldots, z_N) \in \mathbb{C}^{N\times N}$ as the diagonal matrix whose entries are given by $D_{ij} = z_i \delta_{ij}$. A *switching matrix* M is a diagonal matrix whose diagonal entries are all either 1 or -1. Two matrices A, B are said to be *switching equivalent* if there exists a switching matrix M such that $B = M^{-1}AM$. Observe that all switching matrices satisfy $M = M^{-1}$, so we may write $B = MAM$ for any two switching equivalent matrices A and B. A matrix is said to be irreducible if it is not similar to an upper-triangular matrix. The collection of all eigenvalues or *spectrum* of matrix A (also called A-eigenvalues) is denoted as $\sigma(A) = \{\mu_1, \ldots, \mu_N\}$ (repeated eigenvalues appear with their algebraic multiplicity), and we use $\boldsymbol{v} \in \mathbb{C}^N$ and $\boldsymbol{w} \in \mathbb{C}^N$ to represent left and right eigenvectors satisfying $\boldsymbol{v}^t A = \mu \boldsymbol{v}^t$ and $A\boldsymbol{w} = \mu \boldsymbol{w}$, respectively, for some $\mu \in \sigma(A)$. The spectral radius of matrix A is defined as $\rho(A) = \max\{|\mu| : \mu \in \sigma(A)\}$.

An eigenvalue $\mu \in \sigma(A)$ is said to be simple if its algebraic multiplicity is equal to one. An element $\mu^* \in \sigma(A)$ is said to be a *leading eigenvalue* if it is simple and $\mathrm{Re}(\mu^*) \geqslant \mathrm{Re}(\mu)$ for all $\mu \in \sigma(A)$; an element $\mu^* \in \sigma(A)$ is said to be a *strictly leading eigenvalue* if it is simple and $\mathrm{Re}(\mu^*) > \mathrm{Re}(\mu)$ for all $\mu \in \sigma(A) \backslash \{\mu^*, \overline{\mu}^*\}$.

A left or right eigenvector is a *(strictly) leading eigenvector* if it is associated to a (strictly) leading eigenvalue. An $N \times N$ matrix is said to be *in-regular* if it has the all-ones vector $\mathbf{1}_N$ as a right eigenvector. We order the elements $\mu_1, \ldots, \mu_N$ of $\sigma(A)$ decreasingly by their real parts, i.e., $\mathrm{Re}(\mu_j) \geqslant \mathrm{Re}(\mu_{j+1})$ for all $j = 1, \ldots, N-1$. Simple conjugate eigenvalues are ordered decreasingly by their imaginary parts. Real repeated eigenvalues are ordered arbitrarily as consecutive elements; for repeated non-real eigenvalues, we write them in conjugate pairs and order each pair by their imaginary parts. If some real and non-real eigenvalues have equal real parts, real ones come first and then the non-real ones ordered by their imaginary parts. If A has a real strictly leading eigenvalue, then we denote it as $\mu_1 \in \sigma(A)$; if A has a conjugate couple of non-real strictly leading eigenvalues, then we denote them as μ_1 and $\mu_2 = \overline{\mu}_1$, such that $\mathrm{Im}(\mu_1) > 0$.

A $2N$-tuple $\boldsymbol{z}$ may be denoted in *block-wise notation* by $\boldsymbol{z} = (\boldsymbol{x}^t|\boldsymbol{y}^t)^t$, where $\boldsymbol{x}$ and $\boldsymbol{y}$ are N-tuples. The block-wise notation for a $2N \times 2N$ matrix M is $M = \left(\begin{array}{c|c} A & B \\ \hline C & D \end{array}\right)$, where A, B, C, and D are $N \times N$ matrices. Operations between block-wise defined matrices and vectors are such that $\left(\begin{array}{c|c} A & B \\ \hline C & D \end{array}\right)\left(\begin{array}{c} x \\ \hline y \end{array}\right) = \left(\begin{array}{c} Ax+By \\ \hline Cx+Dy \end{array}\right)$.

A *weighted and signed digraph*, or *network*, is defined as a triplet $\mathscr{G} = (V, E, A)$, where $V = \{v_1, \ldots, v_N\}$ is the set of vertices, E is the set of edges connecting the elements in V, and A is the weighted adjacency matrix whose entry A_{jk} determines the weight and the sign of the connection from the kth node to the jth node. A digraph is said to be *strongly connected* if for any two vertices there exists a directed path connecting them, which is equivalent to A being irreducible [15, Theorem 3.2.1]. A weighted digraph is in-regular if there exists $d \in \mathbb{R}$ such that the sum of edge weights into each node is d, which is equivalent to A having $\mathbf{1}_N$ as a right eigenvector.

B. Some useful results

The following theorem (which will be used for bifurcation theoretical computations) follows from methods used for classic biorthogonality results on the eigenvectors of matrices A and A^t [16, Theorem 7.7].

Theorem 1. *Let λ be a simple non-real eigenvalue with right eigenvector $\boldsymbol{w}$. Then there exists a left eigenvector $\boldsymbol{v}$ associated to $\overline{\lambda}$ such that $\boldsymbol{v}^t\boldsymbol{w} = 0$ and $\overline{\boldsymbol{v}}^t\boldsymbol{w} \neq 0$.*

Our main results will largely rely on Hopf bifurcation theory. A Hopf bifurcation describes the emergence of limit cycles in a parameterized vector field as a (control) parameter crosses a critical value. The following theorem (from [17, Theorem 3.4.2], [18, Chapter VIII, Proposition 3.3]) formalizes this idea.

Theorem 2. *Suppose that model $\dot{\boldsymbol{x}} = \boldsymbol{f}(\boldsymbol{x}, \alpha)$, $\boldsymbol{x} \in \mathbb{R}^N$, $\alpha \in \mathbb{R}$, has an equilibrium point at $(\boldsymbol{x}_0, \alpha_0)$. If the model Jacobian J at $(\boldsymbol{x}_0, \alpha_0)$ has a simple pair of pure imaginary eigenvalues and all other eigenvalues with negative real parts then there exists a smooth curve of equilibria $(\boldsymbol{x}(\alpha), \alpha)$ such that $\boldsymbol{x}(\alpha_0) = \boldsymbol{x}_0$, and eigenvalues $\lambda(\alpha)$, $\overline{\lambda}(\alpha)$ which are pure imaginary at $\alpha = \alpha_0$ vary smoothly with α. Let $\boldsymbol{v}$ and $\boldsymbol{w}$ be the left and right eigenvectors of J at $(\boldsymbol{x}_0, \alpha_0)$, satisfying $\boldsymbol{v}^t J = i\,|\lambda|\,\boldsymbol{v}^t$ and $J\boldsymbol{w} = -i\,|\lambda|\,\boldsymbol{w}$, $\lambda \neq 0$, such that $\overline{\boldsymbol{v}}^t\boldsymbol{w} = 2$ and $\boldsymbol{v}^t\boldsymbol{w} = 0$. Let $a = \frac{\partial \mathrm{Re}(\lambda)}{\partial \alpha}(\boldsymbol{x_0}, \alpha_0)$ and $b = \frac{1}{16}\mathrm{Re}\left(\left\langle \boldsymbol{v}, (\mathrm{d}^3\boldsymbol{f})_{\boldsymbol{x}_0,\alpha_0}(\boldsymbol{w}, \boldsymbol{w}, \overline{\boldsymbol{w}})\right\rangle\right)$. If $a > 0$ then for α sufficiently close to α_0, the equilibrium $\boldsymbol{x}(\alpha)$ is stable for $\alpha < \alpha_0$ and unstable for $\alpha > \alpha_0$. Furthermore, if $b < 0$, then for $\alpha > \alpha_0$, there exists a stable limit cycle solution $\boldsymbol{l}_\alpha(t)$ satisfying $\max_{t\in\mathbb{R}} \|\boldsymbol{x}_0 - \boldsymbol{l}_\alpha(t)\| = O\left((\alpha - \alpha_0)^{1/2}\right)$. Conversely, if $b > 0$, then for $\alpha < \alpha_0$ there exists an unstable limit cycle solution $\boldsymbol{l}_\alpha(t)$ satisfying $\max_{t\in\mathbb{R}} \|\boldsymbol{x}_0 - \boldsymbol{l}_\alpha(t)\| = O\left((\alpha_0 - \alpha)^{1/2}\right)$. (The results for $a < 0$ are omitted for conciseness as they won't be used.)*

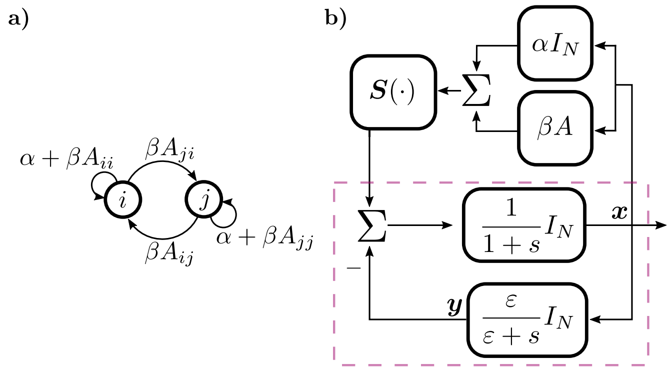

Fig. 1. **a**: Network structure of model (1). Indices $\boldsymbol{i}$, $\boldsymbol{j}$, $\boldsymbol{k}$ denote vertices, and matrix $\boldsymbol{\beta A}$ determines the weights with which vertices influence one another. **b**: block diagram representation. Vector $\boldsymbol{x}$ is the system output. Vector $\boldsymbol{y}$ is a lagged version of $\boldsymbol{x}$. The blue dashed box indicates the linear and local system component. The blocks outside the dashed blue box are nonlinear and networked.

Figure 3 illustrates this theorem for the case $a > 0, b < 0$.

III. A SLOW-FAST NEUROMORPHIC COUPLED OSCILLATOR MODEL OF RHYTHMOGENESIS

Consider a $2N$-dimensional dynamical system

$$\dot{x}_j = -x_j - y_j + S\left(\alpha x_j + \beta \sum_{k=1}^{N} A_{jk} x_k\right), \tag{1a}$$

$$\dot{y}_j = \varepsilon(x_j - y_j), \qquad j = 1, \ldots, N, \tag{1b}$$

where $0 < \varepsilon \ll 1$ is a small positive time constant and S is a locally odd sigmoid. Figure 1a shows the network structure of model (1) and Figure 1b its block diagram representation. Observe the distinct nature of variables x_j and y_j: while the former is the *output* of node j that is transmitted through the network graph, the latter provides distributed *slow negative feedback* on x_j. As we will see, the distributed slow negative feedback provided by the y_js turns nonlinear network interactions mediated by the x_js into robust and easily controllable network oscillations.

Matrix $A \in \mathbb{R}^{N \times N}$ is the adjacency matrix for a network $\mathscr{G}$ with vertices $V = \{1, \ldots, N\}$. Parameter $\alpha \geqslant 0$ models the average self-positive feedback, while parameter $\beta \geqslant 0$ tunes the average interaction strength between the nodes. The choice of introducing network-wide parameters α and β is tailored to the need of having well-defined tuning dials (bifurcation parameters) through which one can modulate the network behavior but observe that the model remains general.

The form of model (1) is motivated by neuromorphic engineering applications. The local (node level) and linear component of the model (blue dashed box in Figure 1b) can be realized in standard CMOS analog neuromorphic circuits [8], [19] using either voltage-mode or current-mode low-pass filters. The nonlinear and network components can be realized using either voltage-mode transconductance amplifiers or current-mode nonlinear circuits. A similar architecture, but with three timescales, was used to realize neuromorphic bursting neurons [9].

Model (1) can be represented as $\dot{\boldsymbol{z}} = \boldsymbol{f}(\boldsymbol{z}; \alpha, \beta)$, where vector field $\boldsymbol{f} = (f_1, \dots, f_{2N}) : \mathbb{R}^{2N} \to \mathbb{R}^{2N}$ is defined entry-wise by

$$f_j(\boldsymbol{z}; \alpha, \beta) = -\boldsymbol{z}_j - \boldsymbol{z}_{j+N} + S\left(\alpha \boldsymbol{z}_j + \beta \sum_{k=1}^{N} A_{jk} \boldsymbol{z}_k\right)$$
$$f_{j+N}(\boldsymbol{z}; \alpha, \beta) = \varepsilon(\boldsymbol{z}_j - \boldsymbol{z}_{j+N}), \qquad j = 1, \dots, N.$$

Since S is a locally odd sigmoid, it follows that $x_j = y_j = 0$ for all $j = 1, \dots, N$, or equivalently, $\boldsymbol{z}_0 = (\boldsymbol{0}_N^t | \boldsymbol{0}_N^t)^t$, is always an equilibrium of model (1). Evaluating the Jacobian matrix at this equilibrium readily yields the following block-wise expression for the $2N \times 2N$ matrix $J_0 = J_{\alpha,\beta,A,\varepsilon}(\boldsymbol{0}_N, \boldsymbol{0}_N)$,

$$J_0 := \left(\begin{array}{c|c} (\alpha - 1)I_N + \beta A & -I_N \\ \hline \varepsilon I_N & -\varepsilon I_N \end{array}\right). \tag{2}$$

IV. Control of Rhythmic Networks: Problem Formulation and Results Overview

In this section we introduce the notion of rhythmic profile as a graphical representation of a network rhythmic behavior. We then formulate the main control objectives and informally present the main results.

A. Rhythmic profiles

We say that a network of coupled oscillators is *rhythmic* if its trajectories (at least for some initial conditions) converge to a limit cycle or, in other words, if asymptotically all of its nodes exhibit periodic oscillations with the same period $T > 0$. The *rhythmic profile* of the network is then defined by the amplitudes and phases of the node oscillations. To formalize these ideas, we first introduce the notion of *oscillating function*, a generalization of functions $\sin(\cdot)$ and $\cos(\cdot)$.

Definition 1 (Oscillating function). *A function $r : \mathbb{R} \to \mathbb{R}$ is called oscillating if it is T-periodic, with $T > 0$, and, moreover, there exist $0 < T_{1/2} < T$ such that $r(0) = r(T_{1/2}) = r(T) = 0$, $r(t) > 0$ for $t \in (0, T_{1/2})$, $r(t) < 0$ for $t \in (T_{1/2}, T)$, and its range is normalized such that* $\max\{r(t) : t \in [0,T]\} - \min\{r(t) : t \in [0,T]\} = 2$.

Definition 2 (Rhythmic network and rhythmic profile). *Consider a network $\mathcal{G}$ with vertices $V = \{1, \dots, N\}$. Suppose that the state of each vertex is described by a state variable $\boldsymbol{x}_j \in \mathbb{R}^n$ and that the network state $\boldsymbol{X} = (\boldsymbol{x}_1^t | \cdots | \boldsymbol{x}_N^t)^t$ evolves according to $\dot{\boldsymbol{X}} = \boldsymbol{f}(\boldsymbol{X})$, where $\boldsymbol{f} : \mathbb{R}^{Nn} \to \mathbb{R}^{Nn}$ is smooth. Let $x_{j1} = (\boldsymbol{x}_j)_1$ be the output of node j. We say that the network $\mathcal{G}$ is* rhythmic *if there exist N oscillating functions $r_1, \dots, r_N : \mathbb{R} \to \mathbb{R}$, N amplitudes $\sigma_1, \dots, \sigma_N \in \mathbb{R}$, N phases $\varphi_1, \dots, \varphi_N \in [0, 2\pi)$, and an open set $U \subset \mathbb{R}^{Nn}$, such that the solution $\boldsymbol{X}(t)$ to $\dot{\boldsymbol{X}} = \boldsymbol{f}(\boldsymbol{X})$, $\boldsymbol{X}(0) = \boldsymbol{X}_0$, satisfies $\lim_{t\to\infty} \left| x_{j1}(t) - \sigma_j r_j\left(t + \frac{T\varphi_j}{2\pi}\right)\right| = 0$ for all $j = 1, \dots, N$, whenever $\boldsymbol{X}_0 \in U$. The* rhythmic profile *of $\mathcal{G}$ is the N-tuple $(\sigma_1 e^{i\varphi_1}, \dots, \sigma_N e^{i\varphi_N}) \in \mathbb{C}^N$.*

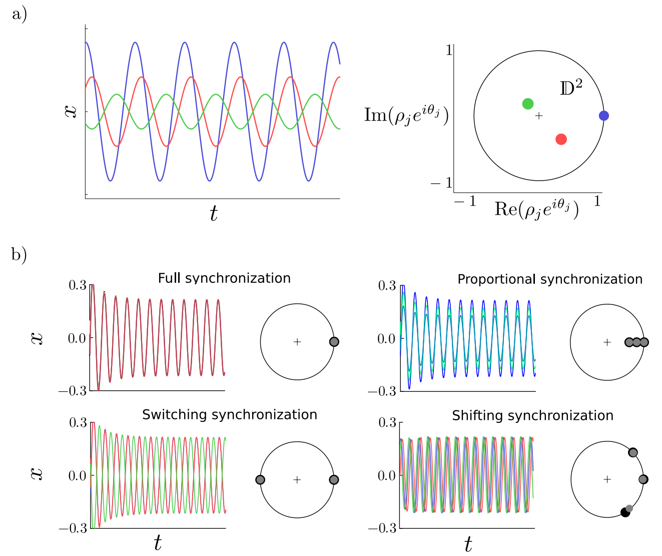

Fig. 2. *a):* Output of a rhythmic network and its amplitude and phase relationships geometrically represented through its relative rhythmic profile in $\mathbb{D}^2$. *b):* Common rhythmic profiles and their prediction. In each panel, the activity pattern of the nodes in a rhythmic network is accompanied by the geometrical representation of its relative rhythmic profile. Black and gray points represent predicted (by our theory) and observed rhythmic profiles, respectively. See text for details.

We can represent the rhythmic profile of a network on the complex unitary disc $\mathbb{D}^2 = \{z \in \mathbb{C} : |z| \leqslant 1\}$ by expressing all amplitudes and phases relative to the amplitude and phase of a the oscillator with largest amplitude.

Definition 3 (Relative rhythmic profile). *Consider a rhythmic network $\mathcal{G}$ and suppose that $\sigma_1 > 0$ and $\sigma_1 \geqslant \sigma_j$ for all $j \neq 1$. Then the* relative rhythmic profile *of $\mathcal{G}$ is defined as the N-tuple $(1, \rho_2 e^{i\theta_2}, \dots, \rho_N e^{i\theta_N}) \in (\mathbb{D}^2)^N$, where $\rho_j = \frac{\sigma_j}{\sigma_1}$ and $\theta_j = \varphi_j - \varphi_1$.*

The relative rhythmic profile can be represented geometrically as the set $\{\rho_1 e^{i\theta_1}, \rho_2 e^{i\theta_2}, \dots, \rho_N e^{i\theta_N}\}$ of N points in the complex unitary disc $\mathbb{D}^2$. Figure 2a shows the relative rhythmic profile of networks with $N = 3$ oscillators. In what follows, when depicting rhythmic profiles, including in Figure 2b, we will omit real and imaginary axes, and solely represent the elements of the profile in a circle representing $\mathbb{D}^2$. The relative rhythmic profile allows for a concise classification of common rhythmic behaviors.

Definition 4 (Common rhythmic profiles). *Let $\mathcal{G}$ be a rhythmic network and $(1, \rho_2 e^{i\theta_2}, \dots, \rho_N e^{i\theta_N})$ denote its relative rhythmic profile. Suppose $r_1 = \cdots = r_N$, i.e., each node is oscillating with the same periodic wave form but possibly different amplitude and phases. We say that the network is (in all points below, $j = 1, \dots, N$):*

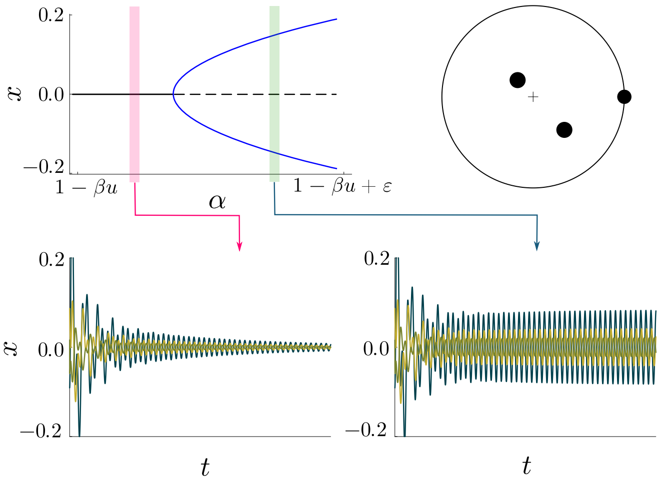

Fig. 3. A Hopf bifurcation triggers the transition from damped to sustained oscillations in model (1). *Top left:* bifurcation diagram of the Hopf bifurcation. Black continuous (dashed) lines represent branches of stable (unstable) equilibria. Blue continuous lines represent branches of stable limit cycles. The loss of stability of the equilibrium point and the appearance of a stable limit cycle are the hallmark of a supercritical Hopf bifurcation. *Top right:* rhythmic profile of an $N = 3$ network. *Bottom:* pre- and post-bifurcation evolution for variables x_j in the same network as the top plots.

- Fully synchronized, *if* $\rho_j = 1$ *and* $\theta_j = 0 \bmod 2\pi$.
- Proportionally synchronized, *if* $\theta_j = 0, \bmod 2\pi$.
- Switching synchronized *if* $\rho_j = 1$ *and* $\theta_j \in \{0, \pi\} \bmod 2\pi$.
- Shifting synchronized *if* $\rho_j = 1$.
- Phase-locked *if the network is rhythmic but none of the above is verified.*

Figure 2 presents the time evolution of the node outputs and the resulting geometric representations of all the kinds of rhythmic profiles introduced in Definition 4.

B. Predicted vs observed relative rhythmic profiles

The representations of the relative rhythmic profiles in Figure 2b, as well as all such representations in the remainder of the paper, show two types of dots associated to each elements of the relative rhythmic profile: a black and a gray one. The black dots represent the predictions obtained with the techniques and results developed in this paper, solely using the spectral properties of the network adjacency matrix. The gray dots represent the measured relative rhythmic profiles. As one can appreciate, for all kinds of rhythmic profiles our predictions matches the observed behavior with very small (often zero) errors.

C. Constructive rhythm control, network structure, and bifurcations

How network structure determines a rhythmic profile is a core question of this work. We will see how in networks of slow-fast coupled oscillators (1) our techniques allows us not only to precisely *analyze* (and thus predict) the emergent rhythmic profile but also to *design* networks to exhibit a desired rhythmic profile. There are indeed two related control problems that we will simultaneously solve:

- *Direct problem:* Can we successfully predict the activity pattern of a given rhythmic network by looking at its adjacency matrix?
- *Inverse problem:* Can we construct an adjacency matrix such that a particular rhythmic profile is attained?

We can solve both problems simultaneously because of the constructive nature of our methods. We develop such a constructive methodology by relying on the Hopf bifurcation theorem, as sketched by Figure 3. To develop some intuition on the importance of the Hopf bifurcation for model (1), let us start by studying the simplest case of uncoupled oscillators, i.e., let's set $A = O_N$. In this case, each node evolves independently according to

$$\begin{aligned} \dot{x} &= -x - y + S(\alpha x), \\ \dot{y} &= \varepsilon(x - y). \end{aligned} \tag{3}$$

The Jacobian matrix of (3) at equilibrium $(x_0, y_0) = (0, 0)$ is $J_0 = \begin{pmatrix} \alpha - 1 & -1 \\ \varepsilon & -\varepsilon \end{pmatrix}$, whose eigenvalues are $\lambda_{1,2} = \dfrac{\alpha - 1 - \varepsilon \pm \sqrt{(\alpha + \varepsilon - 1)^2 - 4\varepsilon}}{2}$, from whence it follows that, whenever $\varepsilon \in (0, 1)$, subsystem (3) undergoes a Hopf bifurcation with bifurcation parameter α at a critical value $\alpha^* = 1 + \varepsilon$. Close to bifurcation, the period is $T = 2\pi\sqrt{\varepsilon(1 - \varepsilon)}^{-1}$.

The case of uncoupled oscillators, although tractable, is not satisfactory from the engineering perspective because phase differences will depend on initial conditions and won't be robustly maintained in the presence of disturbances. In this paper we will develop methods to predict (or design) the emergence of a *networked* Hopf bifurcation that will lead to initial condition-independent and robust rhythmic profiles in a way that is fully determined by network structure. In particular, we will show how the leading eigenstructure of the network adjacency matrix fully determines the emergent rhythmic profile.

D. Slow-fast structure is necessary for constructive rhythmic control

We finish this section by contrasting the predictability (and thus controllability) of rhythms achieved in the slow-fast oscillator network (1) with that achieved using common oscillators models not exhibiting a slow-fast structure. Only in the former does the leading eigenstructure of the network adjacency matrix faithfully predict the emergent rhythmic profile.

The Stuart-Landau oscillator, also known as Andronov-Hopf oscillator, is a commonly used model in network oscillation studies [20]–[27]. Its dynamics are defined as a truncated normal form [17, Equation (3.4.8)] of the Andronov-Hopf bifurcation [28]. As such, only a few parameters are needed to determine the appearance and stability of limit cycles. The most important feature distinguishing oscillator networks based on the Stuart-Landau oscillator from our slow-fast oscillator network (3)

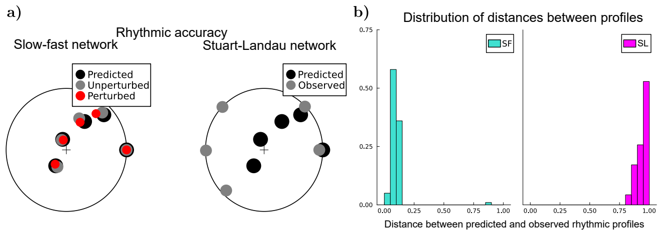

Fig. 4. Accuracy of rhythmic profile prediction in networks where self evolution is either slow-fast (SF) or Stuart-Landau (SL). *Panel a):* predicted (black dots) and measured (gray dots) rhythmic profiles of two $N = 5$ networks with the same adjacency matrix but either SF or SL dynamics. The SF network case also shows the rhythmic profiles under disturbances (red dots). *Panel b):* histogram for the distribution of the distances between predicted an observed rhythmic profiles in one hundred randomly generated networks with $N = 5$ and either SF or SL dynamics. The networks were built using the algorithm described in Section IX for random amplitudes and phases.

is the lack of timescale separation between the x and y variables. Consider a network of Stuart-Landau oscillators

$$\begin{aligned}\dot{x}_j &= \kappa x_j - y_j + \sigma x_j(x_j^2 + y_j^2) + S\left(\beta \sum_{k=1}^{N} A_{jk} x_k\right), \\ \dot{y}_j &= x_j + \kappa y_j + \sigma y_j(x_j^2 + y_j^2).\end{aligned} \tag{4}$$

Parameter $\sigma \in \{-1, 1\}$ determines the stability of the network limit cycle, and $\kappa \in \mathbb{R}$ is the bifurcation parameter, which controls the transition from a stable to an unstable equilibrium point at origin. In virtue of Theorem 2, by choosing $\sigma = -1$ and $\kappa > 0$, we guarantee the existence of stable limit cycles.

Figure 4a shows an example of a relative rhythmic profile as predicted by the leading eigenstructure of the network adjacency matrix (black dots) and as measured (gray dots) in a network of slow-fast oscillators (1) (left) and in a network of Stuart-Landau oscillators (right). Clearly, only in the former do the predictions match observations. Furthermore, rhythmic profiles are robust in networks of slow-fast oscillators, as illustrated by the red dots in Figure 4a (left), which were measured after having added small random perturbations to all the weights of the adjacency matrix.

We further characterized the difference in rhythm predictability of the slow-fast versus Stuart-Landau coupled oscillator models by generating one hundred random networks and by computing the resulting distances between the predicted and observed rhythmic profiles. Figure 4b summarizes this analysis. It reveals that distances are heavily centered around small values (good predictability) for the slow-fast model but around large values (bad predictability) for the Stuart-Landau model.

V. A FAST DOMINANCE ASSUMPTION

The key ingredients of our approach are the slow-fast nature of the oscillators and the following assumption.

Assumption 1. *The adjacency matrix A in model* (1) *has a strictly leading real eigenvalue $\mu_1 > 0$ or strictly leading complex conjugate eigenvalues $\mu_1, \mu_2 = \overline{\mu}_1$,* $\mathrm{Re}(\mu_1) > 0$.

Assumption 1 is key to our approach because it implies that the linearization at the origin of the fast dynamics (1a) of model (1) possesses, for suitable α and β, low-dimensional *dominant dynamics* [29]. Indeed, if A has a strictly leading eigenvalue μ_1, then the Jacobian $J_0^f = (\alpha - 1)I_N + \beta A$ of the fast subsystem, i.e., the upper left block in (2), has also a strictly leading eigenvalue $\alpha - 1 + \beta\mu_1$. Hence, for $\alpha = 1 - \beta\mu_1$ the strictly leading eigenvalue of J^f is purely imaginary, while all non leading eigenvalues have negative real part. Invoking from [29, Proposition 1], the linearization of fast dynamics (1a) is 1-dominant, if μ_1 is real, or 2-dominant, if μ_1 is non-real, with rate $c > 0$ determined by the largest real part of non-leading eigenvalues (dominance analysis of the nonlinear fast dynamics is also possible but more involved and out of scope here).

Dominance implies that (close to the origin) fast dynamics (1a) effectively behave as low-dimensional dynamics, in the sense that they possess an $N-1$ (1-dominance case) or $N-2$ (2-dominance case) dimensional subspace $\mathcal{V}$ such that, if $\boldsymbol{x}(0) \in \mathcal{V}$, $\|\boldsymbol{x}(t)\| \leq Ce^{-\overline{c}t}\|\boldsymbol{x}(0)\|$, where $C > 1$ and $\overline{c} > c$. That is, after a short transient, all persistent dynamical behaviors of the fast dynamics of model (1) happen in a 1 or 2 dimensional complement $\mathcal{H}$ of $\mathcal{V}$, with $\mathcal{H} \oplus \mathcal{V} = \mathbb{R}^N$. The subspace $\mathcal{H}$ is called the *dominant subspace* and it is the real eigenspace associated to $\alpha - 1 + \beta\mu_1$, if μ_1 is real, or to $\alpha - 1 + \beta\mu_1, \alpha - 1 + \beta\overline{\mu}_1$, if μ_1 is not real.

When either α or β are increased and the strictly leading eigenvalue $\alpha - 1 + \beta\mu_1$ crosses the imaginary axis, the fast dynamics become linearly unstable: a bifurcation happens inside the dominant subspace $\mathcal{H}$, at which intrinsically nonlinear (but low-dimensional) dynamical behaviors, like multi-stability or limit cycle oscillations, can emerge.

In the remainder of the paper we will show that the existence of a fast dominant dynamics is inherited by the full slow-fast dynamics (1). Furthermore, the loss of stability of the dominant dynamics of model (1) necessarily leads to limit cycle oscillations through a Hopf bifurcation. The dominant eigenstructure of A fully determines the critical parameter values at which the bifurcation happens as well as the rhythmic profile associated to the emerging limit cycles, thus providing a constructive methodology for rhythmic network control.

A. Sufficient conditions for fast dominance

A well known sufficient condition for the existence of a strictly leading real eigenvalue $\mu_1 = \sigma(A) > 0$ with a positive eigenvector $\boldsymbol{w}_1$ is the Perron-Frobenius theorem [30, Theorem 8.4.4]. The Perron-Frobenius theorem, which applies to matrices with non-negative entries, was generalized to matrices with mixed-sign entries in [31]. The second generalization stems from the notion of (structurally) balanced networks [32]–[34]. The adjacency matrix associated to a structurally balanced network possesses a strictly leading real positive eigenvalue but this eigenvalue is neither guaranteed to be the spectral radius of the matrix nor is the corresponding eigenvector guaranteed to be positive. A summary of conditions under which a graph is defined by an adjacency matrix with a strictly leading real positive eigenvalue can be found in [35, Lemma 2.2]. To the best of the authors' knowledge, no general conditions were ever proved for the existence of a strictly leading complex conjugate eigenvalue pair.

VI. Some linear algebraic definitions and results

We start by showing how spectral properties of Jacobian matrix J_0 in Equation (2) are determined by those of adjacency matrix A, and vice versa. The technical proofs of the results in this section are provided in Appendix I.

A. Spectral relationships between the Jacobian and the adjacency matrix

We start by deriving formulae to compute the $2N$ J_0-eigenvalues in terms of the N A-eigenvalues. We also show that the J_0-eigenvectors, both left and right, inherit the structure of corresponding A-eigenvectors.

Lemma 1. *$\mu \in \sigma(A)$ if and only if there exists $\lambda \in \sigma(J_0)$ such that*

$$\lambda^2 + (1 + \varepsilon - \alpha - \beta\mu)\lambda + \varepsilon(2 - \alpha - \beta\mu) = 0, \tag{5}$$

or, equivalently,

$$\mu = \frac{1 - \alpha + \lambda + \frac{\varepsilon}{\varepsilon+\lambda}}{\beta}. \tag{6}$$

Moreover, for any $\mu \in \sigma(A)$, if $\boldsymbol{w}_x \in \mathbb{C}^N$ is an associated right A-eigenvector, then $\boldsymbol{w} = (\boldsymbol{w}_x^t | \frac{\varepsilon}{\varepsilon+\lambda}\boldsymbol{w}_x^t)^t \in \mathbb{C}^{2N}$ is a right J_0-eigenvector associated to $\lambda \in \sigma(J_0)$ satisfying condition (5)*. Conversely, for any $\lambda \in \sigma(J_0)$, if $\boldsymbol{w} = (\boldsymbol{w}_x^t | \boldsymbol{w}_y^t)^t \in \mathbb{C}^{2N}$ is the associated right J_0-eigenvector then necessarily*

$$A\boldsymbol{w}_x = \mu\boldsymbol{w}_x, \qquad \boldsymbol{w}_y = \tfrac{\varepsilon}{\varepsilon+\lambda}\boldsymbol{w}_x, \tag{7}$$

where $\mu \in \sigma(A)$ satisfies condition (6)*.*

Lemma 2. *For any $\mu \in \sigma(A)$, if $\boldsymbol{v}_x \in \mathbb{C}^N$ is an associated left A-eigenvector then $\boldsymbol{v} = (\boldsymbol{v}_x^t | \frac{-1}{\varepsilon+\lambda}\boldsymbol{v}_x^t)^t \in \mathbb{C}^{2N}$ is a left J_0-eigenvector associated to $\lambda \in \sigma(J_0)$ satisfying condition* (5)*. Conversely, for any $\lambda \in \sigma(J_0)$, if $\boldsymbol{v} = (\boldsymbol{v}_x^t | \boldsymbol{v}_y^t)^t \in \mathbb{C}^{2N}$ is the associated left J_0-eigenvector then necessarily*

$$\boldsymbol{v}_x^t A = \mu\boldsymbol{v}_x^t, \qquad \boldsymbol{v}_y = \tfrac{-1}{\varepsilon+\lambda}\boldsymbol{v}_x, \tag{8}$$

where $\mu \in \sigma(A)$ satisfies condition (6)*.*

B. Further characterization of the spectral properties of the Jacobian matrix

Given $\mu = u + iv \in \sigma(A)$, we denote the two J_0-eigenvalues associated to μ guaranteed by Lemma 1 as $\nu_\mu^+(\alpha,\beta,\varepsilon) = \Phi_\mu^+(\alpha,\beta,\varepsilon) + i\Psi_\mu^+(\alpha,\beta,\varepsilon)$ and $\nu_\mu^-(\alpha,\beta,\varepsilon) = \Phi_\mu^-(\alpha,\beta,\varepsilon) - i\Psi_\mu^-(\alpha,\beta,\varepsilon)$, where the exact expressions for real functions Φ_μ^+, Ψ_μ^+, Φ_μ^-, and Ψ_μ^- are obtained through the formulae for the principal roots of complex numbers and are given by (9), where $c = \alpha + \beta u - 1 - \varepsilon$ and $d = \mathrm{sgn}(\beta v(\alpha + \beta u - 1 + \varepsilon))$. Observe that $\Phi_\mu^- \leqslant \Phi_\mu^+$.

Definition 5 (**Associated eigenvalues**)**.** *Let $\mu \in \sigma(A)$ be an A-eigenvalue. Then for any $\alpha \in \mathbb{R}$, $\beta \in \mathbb{R}$, and $\varepsilon \geqslant 0$, the two J_0-eigenvalues $\nu_\mu^+(\alpha,\beta,\varepsilon)$, $\nu_\mu^-(\alpha,\beta,\varepsilon)$ are called the J_0-eigenvalues associated to μ.*

To simplify the notation, in the sequel we drop the dependence of functions $\nu_\mu^\pm$ on parameters α, β, and ε. Recall that the elements $\mu_1, \dots, \mu_N$ of $\sigma(A)$ are ordered decreasingly by their real parts (see Section II). We use $\nu_j^\pm$ as a shorthand for $\nu_{\mu_j}^\pm$. The following lemma provides conjugation relationships between ν_j^- and ν_j^+.

Lemma 3. *Let $\mu_j \in \sigma(A)$, for $j \in \{1, \dots, N\}$, and ν_j^-, ν_j^+ denote its associated J_0-eigenvalues as in Definition 5. Then the following hold for small enough values of $\varepsilon > 0$.*
a) If $\mu_j \in \mathbb{R}$ and $\{\nu_j^-, \nu_j^+\} \subset \mathbb{R}$, then $\nu_j^- < \nu_j^+$.
b) If $\mu_j \in \mathbb{R}$ and $\{\nu_j^-, \nu_j^+\} \subset \mathbb{C}\backslash\mathbb{R}$, then $\nu_j^- = \overline{\nu}_j^+$.
c) If $\mu_j \in \mathbb{C}\backslash\mathbb{R}$, $j < N$, then $\nu_{j+1}^+ = \overline{\nu}_j^+$ and $\nu_{j+1}^- = \overline{\nu}_j^-$.

VII. Slow-fast leading eigenstructure, dominant dynamics, and their parameter sensitivity

In this section we use Assumption 1 to characterize the leading eigenstructure of J_0, provided knowledge of the leading eigenstructure of A. In particular, we provide conditions on α, β, ϵ under which the J_0-eigenvalues $\nu_1^\pm$ associated to a strictly leading real A-eigenvalue μ_1 or the J_0-eigenvalues ν_1^+, ν_2^+ associated to a strictly leading complex conjugate A-eigenvalues $\mu_1, \mu_2 = \overline{\mu}_1$ have zero real part, while all the other J_0-eigenvalues have negative real part. In other words, we show how the leading eigenstructure of A and the resulting (linearized) fast dominant dynamics (see Section V) map to the leading eigenstructure of J_0 and to a (linearized) 2-dominant dynamics for the full slow-fast dynamics (1). Finally, we characterize how the parameter variations affect the leading eigenvalues of J_0, which will be instrumental for bifurcation analysis. Proofs of the technical results in this section are provided in Appendix I.

A. Existence of critical parameter values for a real leading eigenvalue

We start by guaranteeing that for the strictly leading A-eigenvalue with positive real part $\mu_1 \in \sigma(A)$ there exists a smooth relationship between parameters $(\alpha, \beta, \varepsilon)$ such that the associated J_0-eigenvalues are purely imaginary complex conjugates.

Lemma 4. *Let the strictly leading A-eigenvalue μ_1 be real. Let also*

$$\alpha_{\beta,1}(\varepsilon) = 1 + \varepsilon - \beta\mu_1. \tag{10}$$

Then for small enough $\varepsilon \geqslant 0$, $\beta \in (0, \frac{1}{\mu_1})$, and $\alpha = \alpha_{\beta,1}(\varepsilon)$, the associated J_0-eigenvalues ν_1^- and ν_1^+ are given by

$$\nu_1^\pm = \pm i\sqrt{\varepsilon(1 - \varepsilon)}. \tag{11}$$

Thus, $\lim_{\varepsilon\to 0} |\nu_1^+| = 0$. Moreover, $\frac{\partial \Phi_1^\pm}{\partial \alpha}(\alpha_{\beta,1}(\varepsilon), \beta, \varepsilon) > 0$.

$$
\begin{aligned}
\Phi_\mu^+(\alpha,\beta,\varepsilon) &= \tfrac{c}{2} + \tfrac{1}{2}\sqrt{\frac{\sqrt{((\alpha+\beta u-1-\varepsilon)^2-\beta^2v^2-4\varepsilon(2-\alpha-\beta u))^2+4\beta^2v^2(\alpha+\beta u-1+\varepsilon)^2}+(\alpha+\beta u-1-\varepsilon)^2-\beta^2v^2-4\varepsilon(2-\alpha-\beta u)}{2}},\\
\Psi_\mu^+(\alpha,\beta,\varepsilon) &= \tfrac{\beta v}{2} + \tfrac{d}{2}\sqrt{\frac{\sqrt{((\alpha+\beta u-1-\varepsilon)^2-\beta^2v^2-4\varepsilon(2-\alpha-\beta u))^2+4\beta^2v^2(\alpha+\beta u-1+\varepsilon)^2}-(\alpha+\beta u-1-\varepsilon)^2+\beta^2v^2+4\varepsilon(2-\alpha-\beta u)}{2}},\\
\Phi_\mu^-(\alpha,\beta,\varepsilon) &= \tfrac{c}{2} - \tfrac{1}{2}\sqrt{\frac{\sqrt{((\alpha+\beta u-1-\varepsilon)^2-\beta^2v^2-4\varepsilon(2-\alpha-\beta u))^2+4\beta^2v^2(\alpha+\beta u-1+\varepsilon)^2}+(\alpha+\beta u-1-\varepsilon)^2-\beta^2v^2-4\varepsilon(2-\alpha-\beta u)}{2}},\\
\Psi_\mu^-(\alpha,\beta,\varepsilon) &= \tfrac{\beta v}{2} - \tfrac{d}{2}\sqrt{\frac{\sqrt{((\alpha+\beta u-1-\varepsilon)^2-\beta^2v^2-4\varepsilon(2-\alpha-\beta u))^2+4\beta^2v^2(\alpha+\beta u-1+\varepsilon)^2}-(\alpha+\beta u-1-\varepsilon)^2+\beta^2v^2+4\varepsilon(2-\alpha-\beta u)}{2}}.
\end{aligned}
\tag{9}
$$

Lemma 5. *Let the strictly leading A-eigenvalue μ_1 be real. Let also*

$$\beta_{\alpha,1}(\varepsilon) = \frac{1+\varepsilon-\alpha}{\mu_1}, \tag{12}$$

Then for small enough values of $\varepsilon \geqslant 0$, $\alpha \in (0,1)$, and $\beta = \beta_{\alpha,1}(\varepsilon)$, the associated J_0-eigenvalues ν_1^- and ν_1^+ are given by (11). Moreover, $\frac{\partial \Phi_1^\pm}{\partial \beta}(\alpha, \beta_{\alpha,1}(\varepsilon), \varepsilon) > 0$.

B. Existence of critical parameter values for a non-real leading eigenvalue

For analogous results in the non-real μ_1 case we rely on existence results (derived from the implicit function theorem), and thus we do not arrive at explicit expressions for $\alpha_{\beta,1}$ and $\beta_{\alpha,1}$. Furthermore, in the non-real μ_1 case the conjugate J_0-eigenvalue to ν_1^+ is ν_2^+ instead of ν_1^-.

Lemma 6. *Let the strictly leading A-eigenvalue $\mu_1 = u + iv$ be non-real with positive real part. Then for small enough values of $\varepsilon \geqslant 0$ and $\beta \in (0, \frac{1}{\mathrm{Re}(\mu_1)})$ there exists a differentiable function $\alpha_{\beta,1}(\varepsilon)$, satisfying $\alpha_{\beta,1}(0) = 1 - \beta u$ such that, for $\alpha = \alpha_{\beta,1}(\varepsilon)$, the associated J_0-eigenvalues ν_1^+ and ν_2^+ are given by*

$$\nu_{1,2}^+ = \pm i \left(\frac{\beta v}{2} + \frac{1}{2}\sqrt{\beta^2 v^2 + 4\varepsilon(2-\alpha-\beta u)} \right), \tag{13}$$

and, in particular, $\lim_{\varepsilon\to 0} \left|\nu_{1,2}^+\right| = \beta \mathrm{Im}(\mu_1)$. Furthermore,

$$1 - \beta\mathrm{Re}(\mu_1) - \varepsilon < \alpha_{\beta,1}(\varepsilon) < 1 - \beta\mathrm{Re}(\mu_1) + \varepsilon, \tag{14}$$

$$\alpha_{\beta,1}(\varepsilon) = 1 - \beta\mathrm{Re}(\mu_1) + O(\varepsilon^2), \tag{15}$$

and $\frac{\partial \Phi_{1,2}^+}{\partial \alpha}(\alpha_{\beta,1}(\varepsilon), \beta, \varepsilon) > 0$.

Lemma 7. *Let the strictly leading A-eigenvalue μ_1 be non-real with positive real part. Then for small enough values of $\varepsilon \geqslant 0$ and $\alpha \in (0,1)$ there exists a differentiable function $\beta_{\alpha,1}(\varepsilon)$ satisfying $\beta_{\alpha,1}(0) = \frac{1-\alpha}{\mathrm{Re}(\mu_1)}$, such that, for $\beta = \beta_{\alpha,1}(\varepsilon)$, ν_1^+ and ν_2^+ are given by Equation (13). Furthermore*

$$1 - \alpha - \varepsilon < \mathrm{Re}(\mu_1)\beta_{\alpha,1}(\varepsilon) < 1 - \alpha + \varepsilon, \tag{16}$$

and $\frac{\partial \Phi_{1,2}^+}{\partial \beta}(\alpha, \beta_{\alpha,1}(\varepsilon), \varepsilon) > 0$.

C. Critical value functions

Functions $\alpha_{\beta,1}$ and $\beta_{\alpha,1}$ defined in Lemmata 4 to 7 provide parameter values at which the Jacobian J_0 has purely imaginary leading eigenvalues, corresponding to a Hopf bifurcation of the slow-fast dynamics (1).

Definition 6. *For strictly leading A-eigenvalue μ_1 with positive real part, and $\beta \in (0, \frac{1}{\mathrm{Re}(\mu_1)})$, the function $\alpha_{\beta,1}$ defined in Lemmata 4 and 6 is called the α-*critical value function.

Definition 7. *For strictly leading A-eigenvalue μ_1 with positive real part, and $\alpha \in (0,1)$, the function $\beta_{\alpha,1}$ defined in Lemmata 5 and 7 is called the β-*critical value function.

D. Preservation of dominance near critical values

We now show that for $\alpha = \alpha_{\beta,1}(\varepsilon)$ or $\beta = \beta_{\alpha,1}(\varepsilon)$ dominance of the fast dynamics, as implied by Assumption 1 is inherited by the full slow-fast system (1).

Lemma 8. *Let the strictly leading A-eigenvalue μ_1 be real, and $\alpha_{\beta,1}$ be the α-critical value function as in Definition 6. Then for small enough $\varepsilon > 0$, $\beta \in (0, \frac{1}{\mathrm{Re}(\mu_1)})$, and $\alpha = \alpha_{\beta,1}(\varepsilon)$, the associated J_0-eigenvalues ν_j^- and ν_j^+ have negative real parts, for all $j \in \{2,\dots,k\}$.*

Lemma 9. *Let the strictly leading A-eigenvalue μ_1 be non-real, and $\alpha_{\beta,1}$ be the α-critical value function as in Definition 6. Then for small enough $\varepsilon > 0$, $\beta \in (0, \frac{1}{\mathrm{Re}(\mu_1)})$, and $\alpha = \alpha_{\beta,1}(\varepsilon)$, the associated J_0-eigenvalues ν_1^-, ν_2^-, ν_j^- and ν_j^+ have negative real parts, for all $j \in \{3,\dots,k\}$.*

Lemma 10. *Let the strictly leading A-eigenvalue μ_1 be real, and $\beta_{\alpha,1}$ be the β-critical value function as in Definition 7. Then for small enough $\varepsilon > 0$, $\alpha \in (0,1)$, and $\beta = \beta_{\alpha,1}(\varepsilon)$, the associated J_0-eigenvalues ν_j^- and ν_j^+ have negative real parts, for all $j \in \{2,\dots,k\}$.*

Lemma 11. *Let the strictly leading A-eigenvalue μ_1 be non-real, and $\beta_{\alpha,1}$ be the β-critical value function as in Definition 7. Then for small enough $\varepsilon > 0$, $\alpha \in (0,1)$, and $\beta = \beta_{\alpha,1}(\varepsilon)$, the associated J_0-eigenvalues ν_1^-, ν_2^-, ν_j^- and ν_j^+ have negative real parts, for all $j \in \{3,\dots,k\}$.*

VIII. Constructive rhythmic network control

A. Controlled rhythmogenesis organized by a Hopf bifurcation

We now prove that for $\alpha = \alpha_{\beta,1}(\varepsilon)$ or $\beta = \beta_{\alpha,1}(\varepsilon)$ model (1) undergoes a Hopf bifurcation when α or β is the bifurcation parameter, respectively. We further characterize the dominant subspace $\mathcal{H}$ linearized dynamics at bifurcation, thus providing a description of the emerging rhythmic profile through the *Center Manifold Theorem* [17, Theorem 3.2.1].

Theorem 3. *Consider model* (1)*. Let Assumption 1 hold,* $\beta \in (0, \frac{1}{\mathrm{Re}(\mu_1)})$*, and* $\alpha_{\beta,1}$ *be defined as Definition 6. Then, for* $\varepsilon > 0$ *sufficiently small, the origin is exponentially stable for* $\alpha < \alpha^* = \alpha_{\beta,1}(\varepsilon)$*, exponentially unstable for* $\alpha > \alpha^*$*, and a Hopf bifurcation happens through bifurcation parameter* α *at* $\alpha = \alpha^*$*.*

Proof. By Lemmata 4 and 6, J_0 has a pair of pure imaginary non-real complex eigenvalues $\nu_1^{\pm}$ (if μ_1 is real) or $\nu_{1,2}^{+}$ (if μ_1 is non-real) satisfying $\frac{\partial \mathrm{Re}(\nu_1^+)}{\partial \alpha}(\alpha_{\beta,1}(\varepsilon), \beta, \varepsilon) > 0$ at $\alpha = \alpha_{\beta,1}(\varepsilon)$. By Lemmata 8 and 9, all other J_0-eigenvalues have negative real part. Thus, all the conditions of the Hopf Bifurcation Theorem 2 are satisfied for the case $a > 0$. □

Theorem 4. *Consider model* (1)*. Let Assumption 1 hold,* $\alpha \in (0, 1)$*, and* $\beta_{\alpha,1}(\varepsilon)$ *be defined as Definition 7. Then, for* $\varepsilon > 0$ *sufficiently small, the origin is exponentially stable for* $\beta < \beta^* = \beta_{\alpha,1}(\varepsilon)$*, exponentially unstable for* $\beta > \beta^*$*, and a Hopf bifurcation happens through bifurcation parameter* β *at* $\beta = \beta^*$*.*

Proof. By Lemmata 5 and 7, J_0 has a pair of pure imaginary non-real complex eigenvalues $\nu_1^{\pm}$ (if μ_1 is real) or $\nu_{1,2}^{+}$ (if μ_1 is non-real) satisfying $\frac{\partial \mathrm{Re}(\nu_1^+)}{\partial \beta}(\alpha, \beta_{\alpha,1}(\varepsilon), \varepsilon) > 0$ at $\beta = \beta_{\alpha,1}$. By Lemmata 10 and 11, all other J_0-eigenvalues have negative real part. Thus, all the conditions of the Hopf Bifurcation Theorem 2 are satisfied for the case $a > 0$. □

The 2-dominance of the linearized dynamics of model (1) close to the Hopf bifurcation (as implied by Lemmas 8-11) implies that the 2-dimensional *center manifold* [17, Theorem 3.2.1] of the bifurcation is exponentially stable. Thus, the oscillatory behavior of the linearized dynamics inside the dominant subspace $\mathcal{H}$ characterizes the full nonlinear relative rhythmic profile emerging at the Hopf bifurcation (modulo errors of order $O\left((\alpha - \alpha_{\beta,1}(\varepsilon))^2\right)$ or $O\left((\beta - \beta_{\alpha,1}(\varepsilon))^2\right)$ for α or β as bifurcation parameter). Observe that $\mathcal{H}$ is the generalized eigenspace associated to the strictly leading complex eigenvalue pair. We state and prove the following proposition when α is the bifurcation parameter. The β case is analogous.

Proposition 1. *Under the same assumptions as Theorem 3, let* $\alpha = \alpha_{\beta,1}(\varepsilon)$ *and let* $\boldsymbol{w} = (\boldsymbol{w}_x^t|\boldsymbol{w}_y^t)^t$, $A\boldsymbol{w}_x = \mu_1 \boldsymbol{x}$, $\boldsymbol{w}_y = \frac{\varepsilon}{\varepsilon+\nu_1^+}\boldsymbol{w}_x$*, be a right non-zero eigenvector of* J_0 *for the strictly leading purely complex* J_0*-eigenvalue* ν_1^+ *associated to the strictly leading* A*-eigenvalue* μ_1*. Write* $\boldsymbol{w}_x = (\sigma_n e^{i\varphi_n})_{n=1}^N$ *and suppose, without loss of generality, that* $\sigma_1 > 0$ *and* $\sigma_1 \geqslant \sigma_j$ *for all* $j \neq 1$*. Then the solution* $\boldsymbol{z}(t) = (\boldsymbol{x}^t(t)|\boldsymbol{y}^t(t))^t$ *to the linear system* $\dot{\boldsymbol{z}} = J_0\boldsymbol{z}$ *with initial condition* $\boldsymbol{z}(0) = c_1\mathrm{Re}(\boldsymbol{w}) + c_2\mathrm{Im}(\boldsymbol{w})$ *satisfies*

$$\boldsymbol{x}_n(t) = \sigma_n(c_1 \cos(\left|\nu_1^+\right| t + \varphi_n) + c_2 \sin(\left|\nu_1^+\right| t + \varphi_n)) \quad (17)$$

and in particular it corresponds to a relative rhythmic profile with relative amplitudes $\rho_j = \frac{\sigma_j}{\sigma_1}$ *and relative phases* $\theta_j = \varphi_j - \varphi_1$*.*

Proof. Consider complex function $\boldsymbol{\zeta}(t) = e^{\nu_1^+ t}\boldsymbol{w}$ as a solution to the IVP defined by $\dot{\boldsymbol{\zeta}} = J_0\boldsymbol{\zeta}$, $\boldsymbol{\zeta}(\boldsymbol{0}) = \boldsymbol{w}$. By writing $\boldsymbol{\zeta}(t) = (\boldsymbol{\xi}^t(t)|\boldsymbol{\eta}^t(t))^t$, it is possible to find the analytic entry-wise solutions $\boldsymbol{\xi}_n(t) = \sigma_n e^{i(\left|\nu_1^+\right| t + \theta_n)}$ for every $n \in \{1, \dots, N\}$. Now write $\boldsymbol{\zeta}(t) = \mathrm{Re}(\boldsymbol{\zeta})(t) + i\mathrm{Im}(\boldsymbol{\zeta})(t)$. Then the solutions to real linear system $\dot{\boldsymbol{z}} = J_0\boldsymbol{z}$ are generated by $\mathrm{Re}(\boldsymbol{\zeta})(t)$ and $\mathrm{Im}(\boldsymbol{\zeta})(t)$. By hypothesis we have $\boldsymbol{z}(0) = c_1\mathrm{Re}(\boldsymbol{w}) + c_2\mathrm{Im}(\boldsymbol{w})$, and therefore $\boldsymbol{z}(t) = c_1\mathrm{Re}(\boldsymbol{\zeta})(t) + c_2\mathrm{Im}(\boldsymbol{\zeta})(t)$ for every non-negative time. This in turn implies $\boldsymbol{x}(t) = c_1\mathrm{Re}(\boldsymbol{\xi})(t) + c_2\mathrm{Im}(\boldsymbol{\xi})(t)$, from whence (17) follows. □

It is also easy to see, using $\boldsymbol{w}_y = \frac{\varepsilon}{\varepsilon+\nu_1^+}\boldsymbol{w}_x$, that the slow negative feedback variable y_j oscillates with an amplitude that is ρ_ε times the amplitude of the oscillation of x_j and with a phase difference of θ_ε, where $\rho_\varepsilon e^{i\theta_\varepsilon} = \frac{\varepsilon}{\varepsilon+\nu_1^+}$ and, in particular, $\rho_\varepsilon = O(\varepsilon)$.

By the Center Manifold Theorem [17, Theorem 3.2.1], the limit cycle emerging at the Hopf bifurcation lies on a two-dimensional manifold that is tangent to the dominant subspace $\mathcal{H}$ and is a small perturbation of one of the periodic solutions proved in Proposition 1. It follows that the leading eigenstructure of A fully determines the relative rhythmic profile of the network rhythm emerging at the Hopf bifurcation.

B. Stability of rhythmic profiles

In the following theorem we compute the coefficient b in the normal form of the Hopf bifurcation (see Theorem 2), which determines the stability and the parametric region of existence of the limit cycle emerging at the bifurcation. The proof of this theorem is technical and is provided in Appendix I.

Theorem 5. *Under the same assumptions as Theorem 3, let* $\alpha = \alpha_{\beta,1}(\varepsilon)$, $\boldsymbol{v} = (\boldsymbol{v}_x^t|\boldsymbol{v}_y^t)^t$ *be a left non-zero eigenvector of* J_0 *associated to purely complex* J_0*-eigenvalue* ν_1^+*, and* $\boldsymbol{w} = (\boldsymbol{w}_x^t|\boldsymbol{w}_y^t)^t$ *be a right non-zero eigenvector of* J_0 *associated to* $-\nu_1^+$*, such that (see Theorem 1)* $\boldsymbol{v}^t\boldsymbol{w} = 0$ *and* $\overline{\boldsymbol{v}}^t\boldsymbol{w} = 2$*. Then coefficient* b *in Theorem 2 is given by*

$$\begin{aligned} b = & \tfrac{1}{16}\left|1 - \nu_1^+ + \tfrac{\varepsilon}{\varepsilon-\nu_1^+}\right|^2 S'''(0)\cdot \\ & \cdot \mathrm{Re}\left(\left(1 - \nu_1^+ + \tfrac{\varepsilon}{\varepsilon-\nu_1^+}\right)\langle \boldsymbol{v}_x, \boldsymbol{w}_x \odot \boldsymbol{w}_x \odot \overline{\boldsymbol{w}}_x\rangle\right). \end{aligned} \quad (18)$$

When $b < 0$ (supercritical Hopf bifurcation), the limit cycle emerging at the Hopf bifurcation is stable and exists for α or β close to and above their critical values α^* or β^*, respectively. When $b > 0$ (subcritical Hopf bifurcation), the limit cycle emerging at the Hopf bifurcation is unstable

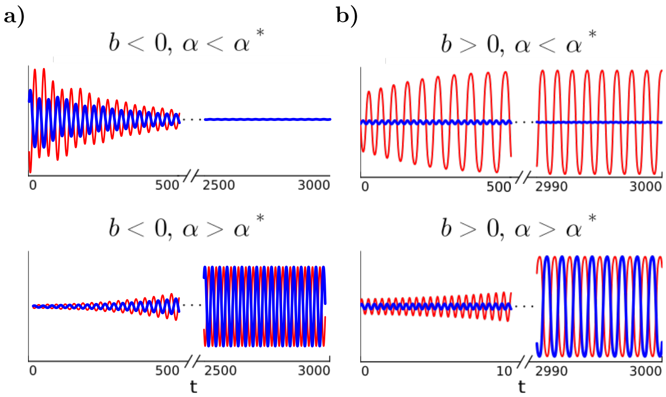

Fig. 5. Dynamical behaviors close to a supercritical vs a subcritical Hopf bifurcation. a) Pre-bifurcation (top) and post-bifurcation (bottom) behaviors for the supercritical case. Pre-bifurcation, all trajectories exhibit damped oscillations converging to the origin. Post-bifurcation, all trajectories converges to a stable limit cycle oscillation emerging at the Hopf bifurcation. b) Pre-bifurcation (top) and post-bifurcation (bottom) behaviors for the subcritical case. Pre-bifurcation, some trajectories exhibit damped oscillations converging to the origin while other trajectories converge toward a stable limit cycle oscillations. The two kinds of trajectories are separated by the stable manifold of an unstable limit cycle emerging at the Hopf bifurcation. Post-bifurcation, all trajectories converge to the stable limit cycle oscillation.

and exists for α or β close to and below their critical values α^* or β^*, respectively. In the subcritical case, the unstable limit cycle is surrounded by a larger amplitude stable limit cycle that persists past the bifurcation point[1]. Figure 5 illustrates the qualitative difference between a supercritical and a subcritical Hopf bifurcation, as predicted by the sign of the computed b coefficient.

We were not able to derive general conditions guaranteeing a given sign for b. However, the following corollary (proved in Appendix I) provides a sufficient condition for $b<0$ and therefore a supercritical Hopf bifurcation.

Corollary 1. *If matrix A is such that its strictly leading right eigenvectors are modulus-homogeneous, and $\varepsilon>0$ is small enough, then $b<0$ and the Hopf bifurcation undergone by system (1) as proved in Theorems 3 and 4 is supercritical.*

One important special case of Corollary 1 is when matrix A is switching equivalent (see Section VI) to either a positive in-regular or a non-negative in-regular irreducible matrix $P=MAM$. As P has a positive eigenvector $\mathbf{1}_N$ associated to a positive eigenvalue $d>0$, then Perron-Frobenius theory [30, Theorem 8.4.4 and Exercise 8.4.P21] (see also Section V-A) implies that d is the leading eigenvalue, thus A has a leading eigenvalue d and a leading eigenvector $M\mathbf{1}_N$, which is modulus-homogeneous. By applying Corollary 1, we conclude that the rhythmic profile arising from the bifurcation must be a switching synchronization profile (see Definition 4) determined by the signs of $M\mathbf{1}_N$ and must be stable.

[1]The proof of this fact goes beyond the scope of this paper and involves invoking boundedness of the trajectories of model (1) and computing higher-order derivatives of similar kinds as coefficients a and b in Theorem 2.

IX. Designing rhythmic networks

The results in the previous sections suggest a constructive way to design rhythmic networks with a desired rhythmic profile. Namely, given desired relative amplitudes $\rho_2,\dots,\rho_N\leqslant\rho_1=1$ and desired relative phases $\theta_2,\dots,\theta_N$, it suffices to find an adjacency matrix A such that $\boldsymbol{w}_x=(1,\rho_2e^{i\theta_2},\dots,\rho_Ne^{i\theta_N})$ is its right eigenvector associated to a strictly leading eigenvalue μ_1. Before discussing simple ways to achieve this, let us distinguish two important cases:

i) $\boldsymbol{w}_x\in\mathbb{R}^N$, that is, $\theta_j\in\{0,\pi\}\bmod 2\pi$ for all $j=2,\dots,N$.
ii) $\boldsymbol{w}_x\notin\mathbb{R}^N$, that is, $\theta_j\notin\{0,\pi\}\bmod 2\pi$ for at least one j.

In Case i), the strictly leading A-eigenvalue μ_1 is real and the modulus of the associated strictly leading J_0-eigenvalues $\nu_1^{\pm}$, given by (11), is $O\left(\varepsilon^{1/2}\right)$. This implies that we cannot arbitrarily control the period $T=2\pi\left|\nu_1^{\pm}\right|^{-1}$ of the emerging rhythmic profile, which diverges to infinity as $\varepsilon\to 0$. However, in practice, given a sufficiently large timescale separation, that is, a sufficiently small *fixed* ε, we can achieve a desired period by suitably scaling the model vector field, i.e., by suitably speeding up all the model variables. This problem is absent in Case ii) because μ_1 is not real and, using (11), the modulus of the strictly leading J_0-eigenvalues $\nu_{1,2}^{+}$ is approximately $\beta\mathrm{Im}(\mu_1)>0+O\left(\varepsilon^{1/2}\right)$. Thus, when the leading eigenstructure of A is not real, and therefore relative phases of the emerging rhythm are not constrained to be 0 or π, the emerging rhythm period is approximately $T\approx 2\pi(\beta\mathrm{Im}(\mu_1))^{-1}$, and thus fully controllable by suitably designing μ_1.

We illustrate the construction of matrix A on two specific rhythmic profile control problem: *amplitude control*, as an example of Case i), and *phase control*, as an example of Case ii). We consider the case in which the network topology is unconstrained and discuss extensions to the constrained case in Section X.

A. Rhythm amplitude control

The goal is to achieve a network rhythm in which oscillations are either in-phase or anti-phase, i.e., $\theta_2,\cdots,\theta_N\in\{0,\pi\}\bmod 2\pi$, by different desired relative oscillation amplitudes $\rho_2,\dots,\rho_N$. With an abuse of terminology, we allow the amplitude ρ_j to be negative, which is equivalent to setting $\theta_j=\pi$ (anti-phase oscillation), but still impose the constraint $|\rho_j|\leqslant\rho_1=1$. A simple way to build an adjacency matrix A leading to such a relative rhythmic profile is the following:

1) Let $\boldsymbol{w}_x=(1,\rho_2,\dots,\rho_N)$.
2) Pick $\mu_1>0$, $\mu_2,\dots,\mu_N<\mu_1$, and let $D=\mathrm{diag}(\mu_1,\mu_2,\dots,\mu_N)$.
3) Find an ordered basis $\mathcal{B}=\{\boldsymbol{w}_x,\boldsymbol{u}_2,\dots,\boldsymbol{u}_N\}$ of $\mathbb{R}^N$ and let $Q=(\boldsymbol{w}_x\ \boldsymbol{u}_2\ \cdots\ \boldsymbol{u}_N)$ be the change of variable from the canonical basis of $\mathbb{R}^N$ to $\mathcal{B}$.
4) Define $A=QDQ^{-1}$.

The constructed A has μ_1 as its leading eigenvalue, and $\boldsymbol{w}_x$ as a leading eigenvector. Since $(\boldsymbol{w}_x)_1=1$, a possibility

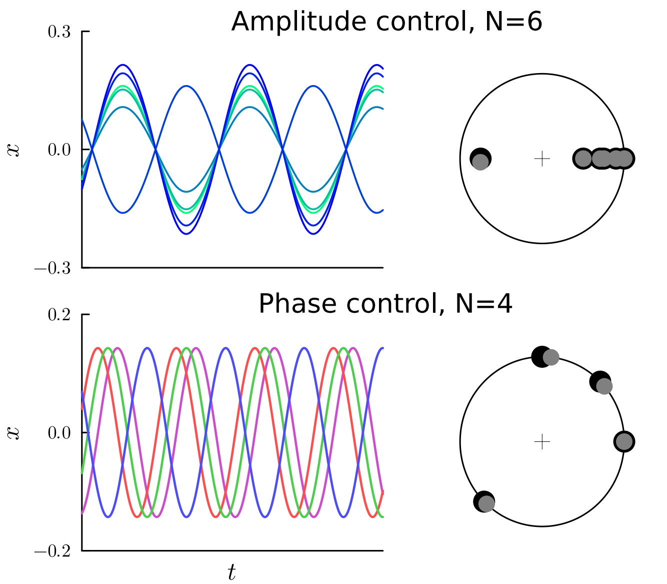

Fig. 6. Examples of controlled rhythmic profiles with matrices built through the algorithm described in this section. *Top:* a real leading eigenvector, with some entries being possibly of opposite signs, results in in-phase or anti-phase oscillations. *Below:* a modulus-homogeneous leading eigenvector where at least one entry is not real leads to a shifting synchronization behavior.

to build the basis $\mathcal{B}$ is to pick $\boldsymbol{u}_j = \boldsymbol{e}_j$, which leads to

$$A = \begin{pmatrix} \mu_1 & 0 & \dots & 0 \\ w_2(\mu_1-\mu_2) & \mu_2 & \dots & 0 \\ \vdots & \vdots & \ddots & \vdots \\ w_N(\mu_1-\mu_N) & 0 & \dots & \mu_N \end{pmatrix}.$$

where $w_j := (\boldsymbol{w}_x)_j$. Such an adjacency matrix corresponds to a star topology, in which the first oscillator drives all the others. Observe that each oscillator has also a self-loop with weight μ_j. The result of this design is illustrated in Figure 6, top.

B. Rhythm phase control

The goal is to achieve a network rhythm in which oscillators have the same amplitude, i.e., $\rho_2 = \cdots = \rho_N = 1$, by non-zero desired relative phases $\theta_2, \dots, \theta_N$. A simple way to build an adjacency matrix A leading to such a relative rhythmic profile is the following:

1) Let $\boldsymbol{w}_x = (1, e^{i\theta_2}, \dots, e^{i\theta_N})$. Observe that, if $\theta_j \notin \{0,\pi\} \bmod 2\pi$ for any $j > 1$, then $\boldsymbol{w}_x$ and $\overline{\boldsymbol{w}}_x$ are linearly independent.
2) Pick $\mu_1 = u_1 + iv_1$ with $u_1, v_1 > 0$, $\mu_2 = \overline{\mu}_1 = u_1 - iv_1$, and $\mu_3, \dots, \mu_N \in \mathbb{R}$, $\mu_j < u_1$. Let $D = \mathrm{diag}(\mu_1, \overline{\mu}_1, \mu_3, \dots, \mu_N)$.
3) Find an ordered basis $\mathcal{B} = \{\boldsymbol{w}_x, \overline{\boldsymbol{w}}_x, \boldsymbol{u}_3, \dots, \boldsymbol{u}_N\}$ of $\mathbb{C}^N$ such that $\boldsymbol{u}_3, \dots, \boldsymbol{u}_N$ are real, and let $Q = (\boldsymbol{w}_x \ \overline{\boldsymbol{w}}_x \ \boldsymbol{u}_3 \ \cdots \ \boldsymbol{u}_N)$ be the change of variable from the canonical basis of $\mathbb{C}^N$ to $\mathcal{B}$.
4) Define $A = QDQ^{-1}$. Note that A is real because D is the complex Jordan form associated to the complex basis $\mathcal{B}$ and Q is the change of variable that put A in its complex Jordan form.

Observe that A has a $\mu_1, \mu_2 = \overline{\mu}_1$ as strictly leading eigenvalues with $\boldsymbol{w}_x$ and $\overline{\boldsymbol{w}}_x$ as strictly leading eigenvectors. It easy to see that for $\theta_2 \notin \{0,\pi\} \bmod 2\pi$, a possibility to build the basis $\mathcal{B}$ is to pick $\boldsymbol{u}_j = \boldsymbol{e}_j$, which leads to adjacency matrix A=

$$\begin{pmatrix} \frac{\mathrm{Im}(\overline{\mu}_1 w_2)}{\mathrm{Im}(w_2)} & \frac{\mathrm{Im}(\mu_1)}{\mathrm{Im}(w_2)} & 0 & \dots & 0 \\ |w_2|^2 \frac{\mathrm{Im}(\overline{\mu}_1)}{\mathrm{Im}(w_2)} & \frac{\mathrm{Im}(\mu_1 w_2)}{\mathrm{Im}(w_2)} & 0 & \dots & 0 \\ \frac{\mathrm{Im}((\overline{\mu}_1-\mu_3) w_2 \overline{w}_3)}{\mathrm{Im}(w_2)} & \frac{\mathrm{Im}((\mu_1-\mu_3) w_3)}{\mathrm{Im}(w_2)} & \mu_3 & \dots & 0 \\ \vdots & \vdots & \vdots & \ddots & \vdots \\ \frac{\mathrm{Im}((\overline{\mu}_1-\mu_N) w_2 \overline{w}_N)}{\mathrm{Im}(w_2)} & \frac{\mathrm{Im}((\mu_1-\mu_N) w_N)}{\mathrm{Im}(w_2)} & 0 & \dots & \mu_N \end{pmatrix}$$

where $w_j := (\boldsymbol{w}_x)_j$. Such an adjacency matrix corresponds to a star topology with a two-node core, in which the first two oscillators are mutually coupled and drive all the others. Observe that each oscillator has also a self-loop. The result of this design is illustrated in Figure 6, bottom.

X. Discussion

We introduced new theoretical tools to design the rhythmic profile of a rhythmic network. Our tools are constructive and can be used for analysis, control, and design. Furthermore, they are developed on a model that is compatible with neuromorphic engineering applications.

Future theoretical development for the extension of the main results include passing from local to global analysis and considering more complicated (e.g., higher-dimensional or with nonlinear slow negative feedback) node dynamics. Another important theoretical development, related to the design strategy described in Section IX, is to consider the case in which the network is structured, i.e., only some edges are present and only the weights of those edges can be tuned to impose a desired leading eigenstructure.

Applications include the hardware realization of model (1) in neuromorphic electronics and the use of the resulting tunable rhythmic controller for locomotion in simple legged robots.

References

[1] E. Marder, D. Bucher, Central pattern generators and the control of rhythmic movements, Curr Biol 11 (23) (2001) R986–R996.
[2] E. Marder, Neuromodulation of neuronal circuits: back to the future, Neuron 76 (1) (2012) 1–11.
[3] S. Grillner, The motor infrastructure: from ion channels to neuronal networks, Nature Reviews Neuroscience 4 (7) (2003) 573–586.
[4] O. Kiehn, Decoding the organization of spinal circuits that control locomotion, Nat Rev Neurosci 17 (4) (2016) 224–38.
[5] M. Golubitsky, I. Stewart, P.-L. Buono, J. Collins, Symmetry in locomotor central pattern generators and animal gaits., Nature 401 (6754) (1999) 693–695.
[6] A. Franci, G. Drion, R. Sepulchre, Robust and tunable bursting requires slow positive feedback, Journal of Neurophysiology 119 (3) (2018) 1222–1234.
[7] T. Y.-C. Tsai, Y. S. Choi, W. Ma, J. R. Pomerening, C. Tang, J. E. Ferrell, Robust, tunable biological oscillations from interlinked positive and negative feedback loops, Science 321 (5885) (2008) 126–129.
[8] E. Chicca, F. Stefanini, C. Bartolozzi, G. Indiveri, Neuromorphic electronic circuits for building autonomous cognitive systems, Proceedings of the IEEE 102 (9) (2014) 1367–1388.

[9] L. Ribar, R. Sepulchre, Neuromodulation of neuromorphic circuits, IEEE Transactions on Circuits and Systems I: Regular Papers 66 (8) (2019) 3028–3040.
[10] J. Duysens, A. Forner-Cordero, A controller perspective on biological gait control: Reflexes and central pattern generators, Annual Reviews in Control 48 (2019) 392–400.
[11] V. Pasandi, H. Sadeghian, M. Keshmiri, D. Pucci, An integrated programmable cpg with bounded output, IEEE Transactions on Automatic Control 67 (9) (2022) 4658–4673.
[12] Z. Chen, T. Iwasaki, Circulant synthesis of central pattern generators with application to control of rectifier systems, IEEE Transactions on Automatic Control 53 (1) (2008) 273–286.
[13] X. Liu, T. Iwasaki, Design of coupled harmonic oscillators for synchronization and coordination, IEEE Transactions on Automatic Control 62 (8) (2017) 3877–3889.
[14] A. J. Ijspeert, A. Crespi, D. Ryczko, J.-M. Cabelguen, From swimming to walking with a salamander robot driven by a spinal cord model, science 315 (5817) (2007) 1416–1420.
[15] R. A. Brualdi, H. J. Ryser, Combinatorial Matrix Theory, 3rd Edition, Cambridge University Press, 1991.
[16] K. B. Datta, Matrix and Linear Algebra Aided with MATLAB, 3rd Edition, PHI Private Learning Limited, 2017.
[17] J. Guckenheimer, P. Holmes, Nonlinear Oscillations, Dynamical Systems, and Bifurcations of Vector Fields, Springer-Verlag New York, 1983.
[18] M. Golubitsky, D. G. Schaeffer, Singularities and Groups in Bifurcation Theory, Vol. 1, Springer-Verlag New York, 1985.
[19] S.-C. Liu, J. Kramer, G. Indiveri, T. Delbruck, R. Douglas, Analog VLSI: circuits and principles, MIT press, 2002.
[20] D. G. Aronson, G. B. Ermentrout, N. Kopell, Amplitude response of coupled oscillators, Physica D: Nonlinear Phenomena 41 (3) (1990) 403–449.
[21] F. C. Hoppensteadt, E. M. Izhikevich, Synaptic organizations and dynamical properties of weakly connected neural oscillators, Biol Cybern 75 (1996) 117–127.
[22] E. M. Izhikevich, Dynamical Systems in Neuroscience, 2nd Edition, The MIT Press, 2007.
[23] N. Tukhlina, M. Rosenblum, A. Pikovsky, J. Kurths, Feedback suppression of neural synchrony by vanishing stimulation, Phys. Rev. E 75 (2007) 011918.
[24] E. Panteley, A. Loría, A. El Ati, Analysis and control of andronov-hopf oscillators with applications to neuronal populations, in: 2015 54th IEEE Conference on Decision and Control (CDC), 2015, pp. 596–601. doi:10.1109/CDC.2015.7402294.
[25] E. Panteley, A. Loria, A. El Ati, On the stability and robustness of stuart-landau oscillators, IFAC-PapersOnLine 48 (11) (2015) 645–650.
[26] K. Premalatha, V. K. Chandrasekar, M. Senthilvelan, M. Lakshmanan, Stable amplitude chimera states in a network of locally coupled stuart-landau oscillators, Chaos 28 (3) (2018) 033110.
[27] S. L. Harrison, H. Sigurdsson, P. G. Lagoudakis, Minor embedding with stuart-landau oscillator networks, Phys. Rev. Res. 5 (2023) 013018.
[28] A. A. Andronov, E. A. Leontovich, I. I. Gordon, A. G. Maier, Theory of Bifurcations of Dynamical Systems on a Plane, Israel Program Sci. Transl., 1971.
[29] F. Forni, R. Sepulchre, Differential dissipativity theory for dominance analysis, IEEE Transactions on Automatic Control 64 (6) (2018) 2340–2351.
[30] R. A. Horn, C. R. Johnson, Matrix Analysis, 2nd Edition, Cambridge University Press, 1985.
[31] D. Noutsos, On perron–frobenius property of matrices having some negative entries, Linear Algebra and its Applications 412 (2-3) (2006) 132–153.
[32] F. Harary, On the notion of balance of a signed graph., Michigan Mathematical Journal 2 (2) (1953) 143–146.
[33] E. D. Sontag, Monotone and near-monotone biochemical networks, Systems and synthetic biology 1 (2) (2007) 59–87.
[34] C. Altafini, Dynamics of opinion forming in structurally balanced social networks, PloS one 7 (6) (2012) e38135.
[35] A. Bizyaeva, A. Franci, N. E. Leonard, Multi-topic belief formation through bifurcations over signed social networks, arXiv preprint arXiv:2308.02755 (2023).

Appendix I
Proofs of lemmata

Lemma 1. *$\mu \in \sigma(A)$ if and only if there exists $\lambda \in \sigma(J_0)$ such that*

$$\lambda^2 + (1 + \varepsilon - \alpha - \beta\mu)\lambda + \varepsilon(2 - \alpha - \beta\mu) = 0, \tag{5}$$

or, equivalently,

$$\mu = \frac{1 - \alpha + \lambda + \frac{\varepsilon}{\varepsilon+\lambda}}{\beta}. \tag{6}$$

Moreover, for any $\mu \in \sigma(A)$, if $\boldsymbol{w}_x \in \mathbb{C}^N$ is an associated right A-eigenvector, then $\boldsymbol{w} = (\boldsymbol{w}_x^t | \frac{\varepsilon}{\varepsilon+\lambda}\boldsymbol{w}_x^t)^t \in \mathbb{C}^{2N}$ is a right J_0-eigenvector associated to $\lambda \in \sigma(J_0)$ satisfying condition (5). Conversely, for any $\lambda \in \sigma(J_0)$, if $\boldsymbol{w} = (\boldsymbol{w}_x^t|\boldsymbol{w}_y^t)^t \in \mathbb{C}^{2N}$ is the associated right J_0-eigenvector then necessarily

$$A\boldsymbol{w}_x = \mu\boldsymbol{w}_x, \qquad \boldsymbol{w}_y = \tfrac{\varepsilon}{\varepsilon+\lambda}\boldsymbol{w}_x, \tag{7}$$

where $\mu \in \sigma(A)$ satisfies condition (6).

Proof. Start by observing that $\lambda^* = -\varepsilon$ does not satisfy quadratic condition (5) for $\varepsilon \neq 0$. We first prove that conditions (5) and (6) are equivalent. Indeed,

$$\beta\mu = 1 - \alpha + \lambda + \tfrac{\varepsilon}{\varepsilon+\lambda} \Leftrightarrow \beta\mu(\varepsilon + \lambda) = (\lambda + 1 - \alpha)(\lambda + \varepsilon) + \varepsilon \Leftrightarrow \beta\mu\lambda + \varepsilon\beta\mu = \lambda^2 + (1 + \varepsilon - \alpha)\lambda + \varepsilon(2 - \alpha).$$

Given $\mu \in \sigma(A)$ and a non-zero right eigenvector $\boldsymbol{w}_x \in \mathbb{C}^N$, consider $\lambda \in \mathbb{C}$ any complex number satisfying (5), or equivalently (6). By proposing $\boldsymbol{w} = (\boldsymbol{w}_x^t|\frac{\varepsilon}{\varepsilon+\lambda}\boldsymbol{w}_x^t)^t \in \mathbb{C}^{2N}$ it suffices to show that $J_0\boldsymbol{w} = \lambda\boldsymbol{w}$. Certainly,

$$\begin{aligned} J_0\boldsymbol{w} &= \left(\begin{array}{c|c} (\alpha-1)I_N + \beta A & -I_N \\ \hline \varepsilon I_N & -\varepsilon I_N \end{array}\right)\left(\begin{array}{c} \boldsymbol{w}_x \\ \hline \frac{\varepsilon}{\varepsilon+\lambda}\boldsymbol{w}_x \end{array}\right) = \left(\begin{array}{c} (\alpha-1)\boldsymbol{w}_x + \beta A\boldsymbol{w}_x - \frac{\varepsilon}{\varepsilon+\lambda}\boldsymbol{w}_x \\ \hline \varepsilon\boldsymbol{w}_x - \frac{\varepsilon^2}{\varepsilon+\lambda}\boldsymbol{w}_x \end{array}\right) \\ &= \left(\begin{array}{c} (\alpha - 1 - \frac{\varepsilon}{\varepsilon+\lambda})\boldsymbol{w}_x + \beta\mu\boldsymbol{w}_x \\ \hline (\varepsilon - \frac{\varepsilon^2}{\varepsilon+\lambda})\boldsymbol{w}_x \end{array}\right) = \left(\begin{array}{c} (\lambda - \beta\mu)\boldsymbol{w}_x + \beta\mu\boldsymbol{w}_x \\ \hline \frac{\varepsilon^2+\varepsilon\lambda-\varepsilon^2}{\varepsilon+\lambda}\boldsymbol{w}_x \end{array}\right) = \left(\begin{array}{c} \lambda\boldsymbol{w}_x \\ \hline \lambda\frac{\varepsilon}{\varepsilon+\lambda}\boldsymbol{w}_x \end{array}\right) = \lambda\boldsymbol{w}. \end{aligned}$$

Conversely, suppose that $\lambda \in \sigma(J_0)$ is an eigenvalue with an associated non-zero eigenvector $\boldsymbol{w} = (\boldsymbol{w}_x^t|\boldsymbol{w}_y^t)^t \in \mathbb{C}^{2N}$ so that $(J_0 - \lambda I_{2N})\boldsymbol{w} = \boldsymbol{0}_{2N}$. This translates to

$$\boldsymbol{0}_{2N} = \left(\begin{array}{c|c} (\alpha - 1 - \lambda)I_N + \beta A & -I_N \\ \hline \varepsilon I_N & -(\varepsilon+\lambda)I_N \end{array}\right)\left(\begin{array}{c} \boldsymbol{w}_x \\ \hline \boldsymbol{w}_y \end{array}\right) = \left(\begin{array}{c} (\alpha - 1 - \lambda)\boldsymbol{w}_x + \beta A\boldsymbol{w}_x - \boldsymbol{w}_y \\ \hline \varepsilon\boldsymbol{w}_x - (\varepsilon+\lambda)\boldsymbol{w}_y \end{array}\right),$$

from whence it is seen that $\lambda^* = -\varepsilon$ is not a right eigenvalue as $\varepsilon \neq 0$. The last equality is equivalent to the system of vector equations

$$\begin{aligned} \beta A\boldsymbol{w}_x &= (1 - \alpha + \lambda + \tfrac{\varepsilon}{\varepsilon+\lambda_1})\boldsymbol{w}_x, \\ \boldsymbol{w}_y &= \tfrac{\varepsilon}{\varepsilon+\lambda}\boldsymbol{w}_x, \end{aligned}$$

so that $\mu = \frac{1}{\beta}(1 - \alpha + \lambda + \frac{\varepsilon}{\varepsilon+\lambda})$ must be an eigenvalue for matrix A. Since this has already been seen to be equivalent to quadratic condition (5), it concludes the proof. □

Lemma 2. *For any $\mu \in \sigma(A)$, if $\boldsymbol{v}_x \in \mathbb{C}^N$ is an associated left A-eigenvector then $\boldsymbol{v} = (\boldsymbol{v}_x^t|\frac{-1}{\varepsilon+\lambda}\boldsymbol{v}_x^t)^t \in \mathbb{C}^{2N}$ is a left J_0-eigenvector associated to $\lambda \in \sigma(J_0)$ satisfying condition (5). Conversely, for any $\lambda \in \sigma(J_0)$, if $\boldsymbol{v} = (\boldsymbol{v}_x^t|\boldsymbol{v}_y^t)^t \in \mathbb{C}^{2N}$ is the associated left J_0-eigenvector then necessarily*

$$\boldsymbol{v}_x^t A = \mu\boldsymbol{v}_x^t, \qquad \boldsymbol{v}_y = \tfrac{-1}{\varepsilon+\lambda}\boldsymbol{v}_x, \tag{8}$$

where $\mu \in \sigma(A)$ satisfies condition (6).

Proof. Given $\mu \in \sigma(A)$ and a non-zero vector $\boldsymbol{v}_x \in \mathbb{C}^N$ such that $\boldsymbol{v}_x^t A = \mu\boldsymbol{v}_x^t$, consider $\lambda \in \mathbb{C}\backslash\{-\varepsilon\}$ any complex number satisfying (6). By proposing $\boldsymbol{v} = (\boldsymbol{v}_x^t|\frac{-1}{\varepsilon+\lambda}\boldsymbol{v}_x^t)^t \in \mathbb{C}^{2N}$, it suffices to show that $\boldsymbol{v}^t J_0 = \lambda\boldsymbol{v}^t$. Certainly,

$$\begin{aligned} \boldsymbol{v}^t J_0 &= (\boldsymbol{v}_x^t|\tfrac{-1}{\varepsilon+\lambda}\boldsymbol{v}_x^t)\left(\begin{array}{c|c} (\alpha-1)I_N + \beta A & -I_N \\ \hline \varepsilon I_N & -\varepsilon I_N \end{array}\right) = \left(\begin{array}{c} (\alpha-1)\boldsymbol{v}_x^t + \beta A\boldsymbol{v}_x^t - \frac{\varepsilon}{\varepsilon+\lambda}\boldsymbol{v}_x^t \\ \hline -\boldsymbol{v}_x^t + \frac{\varepsilon}{\varepsilon+\lambda}\boldsymbol{v}_x \end{array}\right)^t \\ &= \left(\begin{array}{c} (\alpha - 1 - \frac{\varepsilon}{\varepsilon+\lambda})\boldsymbol{v}_x^t + \beta\mu\boldsymbol{v}_x^t \\ \hline (-1 + \frac{\varepsilon}{\varepsilon+\lambda})\boldsymbol{v}_x^t \end{array}\right)^t = \left(\begin{array}{c} (\lambda - \beta\mu)\boldsymbol{v}_x^t + \beta\mu\boldsymbol{v}_x^t \\ \hline \frac{-\lambda}{\varepsilon+\lambda}\boldsymbol{v}_x^t \end{array}\right)^t = \lambda(\boldsymbol{v}_x^t|\tfrac{-1}{\varepsilon+\lambda}\boldsymbol{v}_x^t) = \lambda\boldsymbol{v}^t. \end{aligned}$$

Conversely, suppose that $\lambda \in \sigma(J_0)$ is a left eigenvalue with an associated non-zero eigenvector $\boldsymbol{v} = (\boldsymbol{v}_x^t|\boldsymbol{v}_y^t)^t \in \mathbb{C}^{2N}$ so that $\boldsymbol{v}^t(J_0 - \lambda I_{2N}) = \mathbf{0}_{2N}^t$. This translates to

$$\mathbf{0}_{2N}^t = (\boldsymbol{v}_x^t|\boldsymbol{v}_y^t)\left(\begin{array}{c|c}(\alpha-1-\lambda)I_N+\beta A & -I_N\\ \hline \varepsilon I_N & -(\varepsilon+\lambda)I_N\end{array}\right) = \left(\frac{(\alpha-1-\lambda)\boldsymbol{v}_x^t+\beta A\boldsymbol{v}_x+\varepsilon\boldsymbol{v}_y^t}{-\boldsymbol{v}_x^t-(\varepsilon+\lambda)\boldsymbol{v}_y^t}\right)^t,$$

from whence it is seen that $\lambda^* = -\varepsilon$ is not an eigenvalue. The last equality is equivalent to the vector equation system

$$\beta A\boldsymbol{v}_x = (1-\alpha+\lambda+\tfrac{\varepsilon}{\varepsilon+\lambda})\boldsymbol{v}_x,$$
$$\boldsymbol{v}_y = -\tfrac{1}{\varepsilon+\lambda}\boldsymbol{v}_x,$$

so that $\mu = \frac{1}{\beta}(1-\alpha+\lambda+\frac{\varepsilon}{\varepsilon+\lambda})$ must be an eigenvalue for matrix A. This concludes the proof. □

Lemma 3. *Let $\mu_j \in \sigma(A)$, for $j \in \{1,\ldots,N\}$, and ν_j^-, ν_j^+ denote its associated J_0-eigenvalues as in Definition 5. Then the following hold for small enough values of $\varepsilon > 0$.*
a) If $\mu_j \in \mathbb{R}$ and $\{\nu_j^-,\nu_j^+\} \subset \mathbb{R}$, then $\nu_j^- < \nu_j^+$.
b) If $\mu_j \in \mathbb{R}$ and $\{\nu_j^-,\nu_j^+\} \subset \mathbb{C}\backslash\mathbb{R}$, then $\nu_j^- = \overline{\nu}_j^+$.
c) If $\mu_j \in \mathbb{C}\backslash\mathbb{R}$, $j < N$, then $\nu_{j+1}^+ = \overline{\nu}_j^+$ and $\nu_{j+1}^- = \overline{\nu}_j^-$.

Proof. In the first case we assume that μ_j, as well as the two distinct solutions of

$$\lambda^2 + (1+\varepsilon-\alpha-\beta\mu)\lambda + \varepsilon(2-\alpha-\beta\mu) = 0,$$

are real. This gives straightforward expressions for

$$\nu_j^+ = \frac{\alpha+\beta\mu-1-\varepsilon+\sqrt{(\alpha+\beta\mu-1-\varepsilon)^2-4\varepsilon(2-\alpha-\beta\mu)}}{2},$$
$$\nu_j^- = \frac{\alpha+\beta\mu-1-\varepsilon-\sqrt{(\alpha+\beta\mu-1-\varepsilon)^2-4\varepsilon(2-\alpha-\beta\mu)}}{2}.$$

Now observe that $\nu_j^- < \nu_j^+$ if and only if the discriminant $(\alpha+\beta\mu-1-\varepsilon)^2-4\varepsilon(2-\alpha-\beta\mu)$ is non-zero. If $\alpha+\beta\mu = 1$, then the discriminant is reduced to $\varepsilon^2-4\varepsilon$, which is non-zero for $\varepsilon \in (0,4)$. If $\alpha+\beta\mu \neq 1$, then the discriminant is strictly positive for $\varepsilon = 0$, and therefore it is kept strictly positive for small enough values of ε, thus completing this part of the proof. In the second case it suffices to see that, for $\mu_j \in \mathbb{R}$, eigenvalues $\nu_\mu^\pm = \Phi_\mu \pm i\Psi_\mu$ as given by (9) are complex numbers with real parts equal to $\frac{1}{2}(\alpha+\beta\mu-1-\varepsilon)$, and with imaginary parts of opposite signs. Finally, let $\mu_j = u_j + iv_j$ with $v_j \neq 0$, and by hypothesis $\mu_{j+1} = u_j - iv_j$. By conjugating condition (5), one gets

$$0 = \overline{\lambda}^2 + (1+\varepsilon-\alpha-\beta\overline{\mu}_j)\overline{\lambda} + \varepsilon(2-\beta\overline{\mu}_j-\alpha = \overline{\lambda}^2 + (1+\varepsilon-\alpha-\beta\mu_{j+1})\overline{\lambda} + \varepsilon(2-\alpha-\beta\mu_{j+1}),$$

which concludes that $\overline{\lambda}_j$ satisfies condition (5) written for μ_{j+1}, where λ_j is a solution for condition (5) written for μ_j. It is straightforward to verify from Equations (9) that $\Phi_j^+ = \Phi_{j+1}^+$ as v_j is always squared in them. The sign term d for Ψ_{j+1}^+ is given by

$$\mathrm{sgn}(\beta(v_{j+1})(\alpha+\beta u_{j+1}-1-\varepsilon)) = \mathrm{sgn}(\beta(-v_j)(\alpha+\beta u_j-1-\varepsilon)) = -\mathrm{sgn}(\beta v_j(\alpha+\beta u_j-1-\varepsilon)).$$

Then it is clear that $\Psi_{j+1}^+ = -\Psi_j^+$, which implies that ν_j^+ and ν_{j+1}^+ are conjugates. Equation $\overline{\nu}_j^- = \nu_j^-$ is similarly verified, so we conclude the proof. □

Lemma 4. *Let the strictly leading A-eigenvalue μ_1 be real. Let also*

$$\alpha_{\beta,1}(\varepsilon) = 1+\varepsilon-\beta\mu_1. \tag{10}$$

Then for small enough $\varepsilon \geqslant 0$, $\beta \in (0,\frac{1}{\mu_1})$, and $\alpha = \alpha_{\beta,1}(\varepsilon)$, the associated J_0-eigenvalues ν_1^- and ν_1^+ are given by

$$\nu_1^\pm = \pm i\sqrt{\varepsilon(1-\varepsilon)}. \tag{11}$$

Thus, $\lim_{\varepsilon\to 0}|\nu_1^+| = 0$. Moreover, $\frac{\partial\Phi_1^\pm}{\partial\alpha}(\alpha_{\beta,1}(\varepsilon),\beta,\varepsilon) > 0$.

Proof. When evaluating at $\beta > 0$, $\varepsilon \in (0,1)$, $\alpha = \alpha_{\beta,1}(\varepsilon)$, eigenvalues $\nu_\mu^\pm =$ as given by (9) are reduced to $\pm i\sqrt{\varepsilon(1-\varepsilon)}$, so that ν_1^- and ν_1^+ are conjugate non-real numbers whenever $\varepsilon \in (0,1)$. Discriminant $\Delta = (\alpha+\beta\mu_1-1-\varepsilon)^2-4\varepsilon(2-\beta\mu_1-\alpha)$ reduces to $-4\varepsilon(1-\varepsilon) < 0$ at $\beta > 0$, $\varepsilon > 0$, $\alpha = \alpha_{\beta,1}(\varepsilon)$, so by continuity there must exist an open non-empty subset V of the parameter space where the real part of ν_1^+ is given by $\Phi_1^+ = \frac{1}{2}(\alpha+\beta\mu_1-1-\varepsilon)$, and thus $\frac{\partial\Phi_1^+}{\partial\alpha}(\alpha_{\beta,1}(\varepsilon),\beta,\varepsilon) = \frac{1}{2} > 0$. □

Lemma 5. *Let the strictly leading A-eigenvalue μ_1 be real. Let also*

$$\beta_{\alpha,1}(\varepsilon) = \frac{1+\varepsilon-\alpha}{\mu_1}, \tag{12}$$

Then for small enough values of $\varepsilon \geqslant 0$, $\alpha \in (0,1)$, and $\beta = \beta_{\alpha,1}(\varepsilon)$, the associated J_0-eigenvalues ν_1^- and ν_1^+ are given by (11). Moreover, $\frac{\partial \Phi_1^\pm}{\partial \beta}(\alpha, \beta_{\alpha,1}(\varepsilon), \varepsilon) > 0$.

Proof. Take $\beta_{\alpha,1}(\varepsilon) = \frac{1}{\mu_1}(1+\varepsilon-\alpha)$. Proceed as in Lemma 4, and check that $\frac{\partial \Phi_1^+}{\partial \beta}(\alpha, \beta_{\alpha,1}(\varepsilon), \varepsilon) = \frac{\mu_1}{2} \neq 0$. □

Lemma 6. *Let the strictly leading A-eigenvalue $\mu_1 = u + iv$ be non-real with positive real part. Then for small enough values of $\varepsilon \geqslant 0$ and $\beta \in (0, \frac{1}{\mathrm{Re}(\mu_1)})$ there exists a differentiable function $\alpha_{\beta,1}(\varepsilon)$, satisfying $\alpha_{\beta,1}(0) = 1 - \beta u$ such that, for $\alpha = \alpha_{\beta,1}(\varepsilon)$, the associated J_0-eigenvalues ν_1^+ and ν_2^+ are given by*

$$\nu_{1,2}^+ = \pm i \left(\frac{\beta v}{2} + \frac{1}{2}\sqrt{\beta^2 v^2 + 4\varepsilon(2-\alpha-\beta u)} \right), \tag{13}$$

and, in particular, $\lim_{\varepsilon\to 0} \left|\nu_{1,2}^+\right| = \beta \mathrm{Im}(\mu_1)$. Furthermore,

$$1 - \beta\mathrm{Re}(\mu_1) - \varepsilon < \alpha_{\beta,1}(\varepsilon) < 1 - \beta\mathrm{Re}(\mu_1) + \varepsilon, \tag{14}$$

$$\alpha_{\beta,1}(\varepsilon) = 1 - \beta\mathrm{Re}(\mu_1) + O(\varepsilon^2), \tag{15}$$

and $\frac{\partial \Phi_{1,2}^+}{\partial \alpha}(\alpha_{\beta,1}(\varepsilon), \beta, \varepsilon) > 0$.

Proof. Take $\mu_1 = u + iv$. By formulae (9), equation $\Phi_\mu^+ = 0$ is equivalent to setting $\alpha + \beta u - 1 - \varepsilon$ equal to

$$-\sqrt{\frac{\sqrt{((\alpha+\beta u-1-\varepsilon)^2-\beta^2v^2-4\varepsilon(2-\alpha-\beta u))^2+4\beta^2v^2(\alpha+\beta u-1+\varepsilon)^2}+(\alpha+\beta u-1-\varepsilon)^2-\beta^2v^2-4\varepsilon(2-\alpha-\beta u)}{2}}, \tag{19}$$

which in turn implies

$$(\alpha+\beta u-1-\varepsilon)^2 = \frac{\sqrt{((\alpha+\beta u-1-\varepsilon)^2-\beta^2v^2-4\varepsilon(2-\alpha-\beta u))^2+4\beta^2v^2(\alpha+\beta u-1+\varepsilon)^2}+(\alpha+\beta u-1-\varepsilon)^2-\beta^2v^2-4\varepsilon(2-\alpha-\beta u)}{2} \tag{20}$$

$$\Leftrightarrow (\alpha+\beta u-1-\varepsilon)^2+\beta^2v^2+4\varepsilon(2-\alpha-\beta u) = \sqrt{((\alpha+\beta u-1-\varepsilon)^2-\beta^2v^2-4\varepsilon(2-\alpha-\beta u))^2+4\beta^2v^2(\alpha+\beta u-1+\varepsilon)^2} \tag{21}$$

$$\begin{aligned}
&\Rightarrow ((\alpha+\beta u-1-\varepsilon)^2+\beta^2v^2+4\varepsilon(2-\alpha-\beta u))^2 = ((\alpha+\beta u-1-\varepsilon)^2-\beta^2v^2-4\varepsilon(2-\alpha-\beta u))^2+4\beta^2v^2(\alpha+\beta u-1+\varepsilon)^2\\
&\Leftrightarrow (\alpha+\beta u-1-\varepsilon)^2(\beta^2v^2+4\varepsilon(2-\alpha-\beta u)) = v^2(\alpha+\beta u-1+\varepsilon)^2\\
&\Leftrightarrow \beta^2v^2((\alpha+\beta u-1-\varepsilon)^2-(\alpha+\beta u-1+\varepsilon)^2)+4\varepsilon(\alpha+\beta u-1-\varepsilon)^2(2-\alpha-\beta u) = 0\\
&\Leftrightarrow \varepsilon(\alpha+\beta u-1-\varepsilon)^2(2-\alpha-\beta u)-\beta^2v^2\varepsilon(\alpha+\beta u-1) = 0\\
&\Leftrightarrow (\alpha+\beta u-1-\varepsilon)^2(2-\alpha-\beta u)-\beta^2v^2(\alpha+\beta u-1) = 0
\end{aligned} \tag{22}$$

The resulting polynomial $p(\alpha, \varepsilon)$ in equivalence (22) is cubic in variable α, which guarantees the existence of a real root for every $\varepsilon \in \mathbb{R}$. Additionally, observe that

$$\frac{\partial p}{\partial \alpha}(\alpha,\varepsilon) = (\alpha+\beta u-1-\varepsilon)(5-3\alpha-2\beta u+\varepsilon)-\beta^2v^2 \Rightarrow \frac{\partial p}{\partial \alpha}(1-\beta u, 0) = -\beta^2v^2 \neq 0,$$

so that the Implicit Function Theorem allows us to find a local $\mathscr{C}^1$ solution $(\alpha_{\beta,1}(\varepsilon), \varepsilon)$ defined near point $(1-\beta u, 0)$. Note that when $\alpha = 1-\beta u$, $\varepsilon = 0$, the following expression yields

$$(\alpha+\beta u-1-\varepsilon)^2+\beta^2v^2+4\varepsilon(2-\alpha-\beta u) = \beta^2v^2 > 0;$$

therefore, equations (20) through (22) are actual equivalences along solution $(\alpha_{\beta,1}(\varepsilon), \varepsilon)$. It remains to see that critical value $\alpha = \alpha_{\beta,1}(\varepsilon)$ satisfies $\Phi_1^+ = 0$. To verify this, by once again using the Implicit Function Theorem, derivative $\alpha'_{\beta,1}(\varepsilon)$ is found to be

$$\frac{\mathrm{d}\alpha_{\beta,1}}{\mathrm{d}\varepsilon}(\varepsilon) = -\frac{\frac{\partial p}{\partial \varepsilon}}{\frac{\partial p}{\partial \alpha}}(\alpha_{\beta,1}(\varepsilon),\varepsilon) = \frac{2(\alpha_{\beta,1}(\varepsilon)+\beta u-1-\varepsilon)(2-\alpha_{\beta,1}(\varepsilon)-\beta u)}{(\alpha_{\beta,1}(\varepsilon)+\beta u-1-\varepsilon)(5-3\alpha_{\beta,1}(\varepsilon)-2\beta u+\varepsilon)-\beta^2v^2},$$

thus we get $\alpha'_{\beta,1}(0) = 0$ and $\alpha'_{\beta,1}(\varepsilon) \neq 0$ for small values of $\varepsilon > 0$. This in particular implies the quadratic growth formula (15). By the definition of derivatives, this implies for small enough values of ε that

$$\left|\frac{\alpha_{\beta,1}(\varepsilon)-1+\beta u}{\varepsilon}\right| < 1,$$

and thus, for $\varepsilon > 0$, we get bounds for the growth of function $\alpha_{\beta,1}$, which bounds (14). These inequalities imply that term $\alpha_{\beta,1}(\varepsilon)+\beta u-1-\varepsilon$ is negative for small enough values of $\varepsilon > 0$, so Equation (19) is verified, and thus $\alpha = \alpha_{\beta,1}(\varepsilon)$ satisfies $\Phi_1^+ = 0$. Then for $\beta \in (0, \frac{1}{u})$, $\varepsilon > 0$, $\alpha = \alpha_{\beta,1}(\varepsilon)$ we have $\nu_1^+ = i\Psi_1^+$, which by formulae (9), equivalence (21), and inequality (14) reduces to

$$\Psi_1^+ = \frac{\beta v}{2} + \frac{\mathrm{sgn}(\beta v)}{2}\sqrt{\beta^2v^2+4\varepsilon(2-\alpha-\beta u)}.$$

Recall that we take $v > 0$ in the non-real case. Then having $\Psi_1^+ = 0$ for $\beta \in (0, \frac{1}{u})$, $\varepsilon > 0$, $\alpha = \alpha_{\beta,1}(\varepsilon)$ would imply $\alpha = 2 - \beta u$, which is false for small enough values of $\varepsilon > 0$ as $\alpha_{\beta,1}(0) = 1 - \beta u$, therefore making ν_1^+ a pure imaginary, non-real number. Partially differentiating Φ_μ^+ with respect to α yields

$$\frac{\partial \Phi_1^+}{\partial \alpha}(\alpha, \beta, \varepsilon) = \frac{1}{2} + \frac{1}{4}\frac{\frac{((\alpha+\beta u-1-\varepsilon)^2-\beta^2v^2-4\varepsilon(2-\alpha-\beta u))(\alpha+\beta u-1+\varepsilon)+2\beta^2v^2(\alpha+\beta u-1+\varepsilon)}{\sqrt{((\alpha+\beta u-1-\varepsilon)^2-\beta^2v^2-4\varepsilon(2-\alpha-\beta u))^2+4\beta^2v^2(\alpha+\beta u-1+\varepsilon)^2}}+\alpha+\beta u-1+\varepsilon}{\sqrt{\frac{\sqrt{((\alpha+\beta u-1-\varepsilon)^2-\beta^2v^2-4\varepsilon(2-\alpha-\beta u))^2+4\beta^2v^2(\alpha+\beta u-1+\varepsilon)^2}+(\alpha+\beta u-1-\varepsilon)^2-\beta^2v^2-4\varepsilon(2-\alpha-\beta u)}{2}}}.$$

In order to evaluate the preceding expression at $\beta \in (0, \frac{1}{u})$, $\varepsilon > 0$ and $\alpha = \alpha_{\beta,1}(\varepsilon)$, from equivalence (20), the denominator in the second term reduces to

$$\sqrt{\frac{\sqrt{((\alpha+\beta u-1-\varepsilon)^2-\beta^2v^2-4\varepsilon(2-\alpha-\beta u))^2+4\beta^2v^2(\alpha+\beta u-1+\varepsilon)^2}+(\alpha+\beta u-1-\varepsilon)^2-\beta^2v^2-4\varepsilon(2-\alpha-\beta u)}{2}} = |\alpha + \beta u - 1 - \varepsilon|\,.$$

This term is non-zero by inequality (14) as its argument is negative. The other square root term in $\frac{\partial \Phi_1^+}{\partial \alpha}$ is similarly simplified by equivalence (21). Thus the partial derivative $\frac{\partial \Phi}{\partial \alpha}(\alpha_{\beta,1}(\varepsilon), \beta, \varepsilon)$ yields

$$\frac{1}{2} + \frac{1}{2}\left(\frac{\alpha_{\beta,1}(\varepsilon) + \beta u - 1 + \varepsilon}{1 + \varepsilon - \alpha_{\beta,1}(\varepsilon) - \beta u}\right)\left(\frac{(\alpha_{\beta,1}(\varepsilon) + \beta u - 1 - \varepsilon)^2 + \beta^2 v^2}{(\alpha_{\beta,1}(\varepsilon) + \beta u - 1 - \varepsilon)^2 + \beta^2 v^2 + 4\varepsilon(2 - \alpha_{\beta,1}(\varepsilon) - \beta u)}\right).$$

Inequality (14) guarantees that the second addendum in the previous expression is positive, which concludes that $\frac{\partial \Phi_\mu^+}{\partial \alpha}$ is positive as well at $\beta \in (0, \frac{1}{u})$, $\varepsilon > 0$, $\alpha = \alpha_{\beta,1}(\varepsilon)$. Finally, restrict the domain for $\alpha_{\beta,1}(\varepsilon)$ so that all of the previous assumptions (its definition through the Implicit Function Theorem, and its quadratic growth) hold. ☐

Lemma 7. *Let the strictly leading A-eigenvalue μ_1 be non-real with positive real part. Then for small enough values of $\varepsilon \geqslant 0$ and $\alpha \in (0, 1)$ there exists a differentiable function $\beta_{\alpha,1}(\varepsilon)$ satisfying $\beta_{\alpha,1}(0) = \frac{1-\alpha}{\mathrm{Re}(\mu_1)}$, such that, for $\beta = \beta_{\alpha,1}(\varepsilon)$, ν_1^+ and ν_2^+ are given by Equation (13). Furthermore*

$$1 - \alpha - \varepsilon < \mathrm{Re}(\mu_1)\beta_{\alpha,1}(\varepsilon) < 1 - \alpha + \varepsilon, \tag{16}$$

and $\frac{\partial \Phi_{1,2}^+}{\partial \beta}(\alpha, \beta_{\alpha,1}(\varepsilon), \varepsilon) > 0$.

Proof. Proceed analogously as in Lemma 6. The coefficient for β^3 in the polynomial term in equivalence (22) is $-u(u^2 + v^2)$, which is non-zero by hypothesis. Then it is possible to find real solutions to (22) for β. Partially differentiating the associated polynomial with respect to β now yields

$$\frac{\partial p}{\partial \beta}(\beta, \varepsilon) = u(\alpha + \beta u - 1 - \varepsilon)(5 - 3\alpha - 3\beta u + \varepsilon) - 2\beta v^2(\alpha + \beta u - 1) - \beta^2 u v^2,$$

which implies $\frac{\partial p}{\partial \beta}(\frac{1-\alpha}{u}, 0) = (\alpha - 1)v^2 \neq 0$, so we may use the Implicit Function Theorem to find a $\mathscr{C}^1$ solution to (22), denoted $\beta_{\alpha,1}(\varepsilon)$, and satisfying $\beta_{\alpha,1}(0) = \frac{1-\alpha}{u}$. In can be analogously seen that $\beta'_{\alpha,1}(0) = 0$, therefore guaranteeing inequality

$$\left|\frac{\beta_{\alpha,1}(\varepsilon) - \frac{1-\alpha}{u}}{\varepsilon}\right| < \frac{1}{u}$$

for small enough values of $\varepsilon > 0$, which in turn implies bounds (16). As before, from this last inequality it follows that term $\alpha + \beta_{\alpha,1}(\varepsilon) - 1 - \varepsilon$ is negative, therefore satisfying $\Phi_1^+ = 0$. Then $\nu_1^+ = i\Psi_1^+$, with Ψ_1^+ the same expression as in Lemma 6, only now for $\alpha \in (0, 1)$, $\varepsilon > 0$ and $\beta = \beta_{\alpha,1}(\varepsilon)$. Partial derivative $\frac{\partial \Phi_1^+}{\partial \beta}$ is given by

$$\frac{u}{2} + \frac{1}{4}\frac{\frac{((\alpha+\beta u-1-\varepsilon)^2-\beta^2v^2-4\varepsilon(2-\alpha-\beta u))(u(\alpha+\beta u-1+\varepsilon)-2\beta v^2)+2\beta^2uv^2(\alpha+\beta u-1+\varepsilon)+2\beta v^2(\alpha+\beta u-1+\varepsilon)^2}{\sqrt{((\alpha+\beta u-1-\varepsilon)^2-\beta^2v^2-4\varepsilon(2-\alpha-\beta u))^2+4\beta^2v^2(\alpha+\beta u-1+\varepsilon)^2}}+u(\alpha+\beta u-1+\varepsilon)-2\beta v^2}{\sqrt{\frac{\sqrt{((\alpha+\beta u-1-\varepsilon)^2-\beta^2v^2-4\varepsilon(2-\alpha-\beta u))^2+4\beta^2v^2(\alpha+\beta u-1+\varepsilon)^2}+(\alpha+\beta u-1-\varepsilon)^2-\beta^2v^2-4\varepsilon(2-\alpha-\beta u)}{2}}}.$$

Once again we simplify this expression through equations (20) and (21), and inequality (16). This yields

$$\frac{u}{2} + \frac{1}{2}\frac{((\alpha + \beta u - 1 - \varepsilon)^2 - \beta^2 v^2 - 4\varepsilon(2 - \alpha - \beta u))(u(\alpha + \beta u - 1 + \varepsilon) - \beta v^2) + 2\beta^2 u v^2(\alpha + \beta u - 1 + \varepsilon) + \beta v^2(\alpha + \beta u - 1 + \varepsilon)^2}{(1 + \varepsilon - \alpha - \beta u)((\alpha + \beta u - 1 - \varepsilon)^2 + \beta^2 v^2 + 4\varepsilon(2 - \alpha - \beta u))}.$$

Now observe that

$$\lim_{\varepsilon \to 0^*}((\alpha + \beta_{\alpha,1}(\varepsilon)u - 1 - \varepsilon)^2 - \beta_{\alpha,1}(\varepsilon)^2 v^2 - 4\varepsilon(2 - \alpha - \beta_{\alpha,1}(\varepsilon)u))(u(\alpha + \beta_{\alpha,1}(\varepsilon)u - 1 + \varepsilon) - \beta_{\alpha,1}(\varepsilon)v^2) = \frac{(1 - \alpha)^3 v^2}{u^3}$$

which is positive as we imposed $\alpha \in (0, 1)$. Thus the second addendum in the reduced expression for $\frac{\partial \Phi_1^+}{\partial \beta}(\alpha, \beta_{\alpha,1}(\varepsilon), \varepsilon)$ is positive for small enough values of $\varepsilon > 0$, therefore guaranteeing that $\frac{\partial \Phi_1^+}{\partial \beta}$ is positive as well for $\alpha \in (0, 1)$, $\varepsilon > 0$ and $\beta = \beta_{\alpha,1}(\varepsilon)$, which concludes the proof. ☐

Lemma 8. *Let the strictly leading A-eigenvalue μ_1 be real, and $\alpha_{\beta,1}$ be the α-critical value function as in Definition 6. Then for small enough $\varepsilon > 0$, $\beta \in (0, \frac{1}{\mathrm{Re}(\mu_1)})$, and $\alpha = \alpha_{\beta,1}(\varepsilon)$, the associated J_0-eigenvalues ν_j^- and ν_j^+ have negative real parts, for all $j \in \{2, \dots, k\}$.*

Proof. For the sake of simplicity we introduce the following auxiliary definition. Observe that for $\varepsilon = 0$ the solutions to condition (5) are directly computed as $\alpha + \beta\mu - 1$ and 0. To analytically distinguish them, especially at $\alpha = 1 - \beta\mathrm{Re}(\mu)$, note that one of them varies linearly on α, and the other one is constant. Thus we define the ς-J_0-*eigenvalue* associated to μ_j, denoted as ς_j as the continuous solution to (5) which satisfies $\frac{\partial \mathrm{Re}(\varsigma_j)}{\partial \alpha}(\alpha, 0) = 0$, and the λ-J_0-*eigenvalue* associated to μ_j, denoted as λ_j as the continuous solution to (5) which satisfies $\frac{\partial \mathrm{Re}(\lambda_j)}{\partial \alpha}(\alpha, 0) \neq 0$. A general correspondence between ς_j, λ_j and ν_j^-, ν_j^+ cannot be ascertained for arbitrary values of α, β, and ε.

Denote $\mu_j = u_j + iv_j$ for $j \in \{1, \dots, k\}$. From Lemma 4 we know the explicit definition for the critical value function, $\alpha_{\mu,1}(\varepsilon) = 1 + \varepsilon - \beta\mu_1$. By Lemmata 3 and 4, eigenvalues ν_1^- and ν_1^+ are conjugate non-real numbers for small enough values of $\varepsilon > 0$, $\alpha = \alpha_{\beta,1}(\varepsilon)$. We split the remaining elements in $\sigma(J_0)$ into ς-J_0- and λ-J_0-eigenvalues, as previously defined, $\varsigma_j(\alpha, 0) = 0$, $\lambda_j(\alpha, 0) = \alpha + \beta\mu_j - 1$. Then, for $j \in \{2, \dots, k\}$, it is clear that $\mathrm{Re}(\lambda_j(\alpha_1(0), 0)) = (1 - \beta u_1) + \beta u_j - 1 < 0$. By continuity, this inequality is preserved for small enough values of $\varepsilon > 0$, which takes care of the result for roots λ_j. Now denote ς_j in their Cartesian form, $\varsigma_j = \varphi_j + i\psi_j$. Then the polynomial in (5) is equivalently written

$$(\varphi_j + i\psi_j)^2 + (1 + \varepsilon_j - \alpha_j - \beta u_j - i\beta v_j)(\varphi_j + i\psi_j) + \varepsilon(2 - \beta u_j - i\beta v_j - \alpha),$$

which after developing yields

$$\varphi_j^2 - \psi_j^2 + 2i\varphi_j\psi_j + (1 + \varepsilon - \alpha - \beta u_j)\varphi_j + \beta v_j\psi_j + \varepsilon(2 - \beta u_j - \alpha) + i((1 + \varepsilon - \alpha - \beta u_j)\psi_j - \beta v_j\varphi_j - \beta\varepsilon v_j).$$

The problem of finding the roots for the previously defined quadratic polynomial is equivalent to finding points in the zero level set of function (F_j, G_j), where

$$\begin{aligned} F_j(\alpha, \varepsilon, \varphi_j, \psi_j) &= \varphi_j^2 - \psi_j^2 + (1 + \varepsilon - \alpha - \beta u_j)\varphi_j + \beta v_j\psi_j + \varepsilon(2 - \beta u_j - \alpha), \\ G_j(\alpha, \varepsilon, \varphi_j, \psi_j) &= 2\varphi_j\psi_j + (1 + \varepsilon - \alpha - \beta u_j)\psi_j - \beta v_j\varphi_j - \beta\varepsilon v_j. \end{aligned} \tag{23}$$

The Jacobian determinant of function (F_j, G_j) for subsystem (φ_j, ψ_j) is readily computed as

$$\left|\frac{\partial(F_j, G_j)}{\partial(\varphi_j, \psi_j)}\right| = \begin{vmatrix} 2\varphi_j + 1 + \varepsilon_j - \alpha - \beta u_j & -2\psi_j + \beta v_j \\ 2\psi_j - \beta v_j & 2\varphi_j + 1 + \varepsilon - \alpha - \beta u_j \end{vmatrix} = (2\varphi_j + 1 + \varepsilon - \alpha - \beta u_j)^2 + (2\psi_j - \beta v_j)^2.$$

Recall that $u_1 > u_j$ for every $j \geqslant 2$. Then, at solution $\varepsilon = \varphi = \psi = 0$, $\alpha = 1 - \beta u_1$ and for every $j \geqslant 2$, this determinant reduces to

$$\frac{\partial(F_j, G_j)}{\partial(\varphi_j, \psi_j)} = \beta^2(u_1 - u_j)^2 + \beta^2 v_j^2 \neq 0,$$

and therefore, by virtue of the Implicit Function Theorem, variables φ_j and ψ_j can be expressed as $\mathscr{C}^1$ functions $\Phi_j(\alpha, \varepsilon)$ and $\Psi_j(\alpha, \varepsilon)$ inside the zero level set for values (α, ε) close enough to $(1 - \beta\mu_1, 0)$. Moreover, it is possible to compute their derivatives with respect to ε by

$$\frac{\partial(\Phi_j, \Psi_j)}{\partial\varepsilon} = -\frac{\partial(F_j, G_j)}{\partial(\varphi_j, \psi_j)}^{-1}\left(\frac{\partial(F_j, G_j)}{\partial\varepsilon} + \frac{\partial(F_j, G_j)}{\partial\alpha}\frac{\mathrm{d}\alpha_{\beta,1}}{\mathrm{d}\varepsilon}\right),$$

where the second term inside the parentheses is given by the Chain Rule as $\alpha = \alpha_{\beta,1}(\varepsilon)$ varies as a function of $\varepsilon > 0$. Evaluating at $(1 - \beta\mu_1, 0, 0, 0)$ yields

$$\frac{\partial(\Phi_j, \Psi_j)}{\partial\varepsilon}(1 - \beta u_1, 0) = \frac{-1}{\beta^2(u_1 - u_j)^2 + \beta^2 v_j^2}\begin{pmatrix} \beta u_1 - \beta u_j + \beta^2(u_1 - u_j)^2 + \beta^2 v_j^2 - 0 \\ \beta v_j - 0 \end{pmatrix},$$

from whence it follows that $\frac{\partial\Phi_j}{\partial\varepsilon} < 0$ in a vicinity of $(1 - \beta\mu_1, 0)$. As $\Phi_j(\alpha, 0) = 0$, this implies that $\mathrm{Re}(\varsigma_j) < 0$ for small enough values of $\varepsilon > 0$ and $\alpha = \alpha_{\beta,1}(\varepsilon)$, for every $j \geqslant 2$, thus proving the desired result. □

Lemma 9. *Let the strictly leading A-eigenvalue μ_1 be non-real, and $\alpha_{\beta,1}$ be the α-critical value function as in Definition 6. Then for small enough $\varepsilon > 0$, $\beta \in (0, \frac{1}{\mathrm{Re}(\mu_1)})$, and $\alpha = \alpha_{\beta,1}(\varepsilon)$, the associated J_0-eigenvalues ν_1^-, ν_2^-, ν_j^- and ν_j^+ have negative real parts, for all $j \in \{3, \dots, k\}$.*

Proof. Recall that Lemma 3 guarantees that $\overline{\nu}_1^- = \nu_2^-$ and $\overline{\nu}_1^+ = \nu_2^+$. We proceed analogously as in Lemma 8, which proves the result for associated eigenvalues ν_j^- and ν_j^+, that is, for ς_j and λ_j, for $j \in \{3, \dots, k\}$. Now we have to prove that $\Phi_1^- = \Phi_2^-$ is negative as well. First observe that the expression for Ψ_1^+ found in Lemma 6 guarantees that ν_1^+ is a λ-eigenvalue, therefore making ν_1^- a ς-eigenvalue, $\nu_1^-(\alpha, 0) = 0 + 0i$. When applying the Implicit Function Theorem to zero level set-condition (23) for $j \in \{1,2\}$, at solution $(\alpha, \varepsilon, \phi_1, \psi_1) = (1-\beta u_1, 0, 0, 0)$, the Jacobian determinant is seen to be

$$\frac{\partial(F_1, G_1)}{\partial(\varphi_1, \psi_1)}(1-\beta u_1, 0) = \beta^2(u_1-u_1)^2 + \beta^2 v_1^2 = \beta^2 v_1^2 \neq 0$$

since $\mu_1 = u_1 + iv_1 \notin \mathbb{R}$, so that $v_1 \neq 0$, and $\beta > 0$. Recall from (15) that $\alpha'_{\beta,1}(0) = 0$ in the non-real case. Now, differentiating Φ_1 with respect to ε yields

$$\frac{\partial(\Phi_1, \Psi_1)}{\partial\varepsilon}(1-\beta u_1, 0) = \frac{-1}{\beta^2 v_1^2}\begin{pmatrix} \beta^2 v_1^2 - \alpha_1'(0)(0+\varphi_1) \\ \beta v_1 - \alpha_1'(0)\psi_1 \end{pmatrix} = \begin{pmatrix} -1 \\ -\frac{1}{\beta v_1} \end{pmatrix},$$

and thus $\frac{\partial \Phi_1}{\partial \varepsilon}(1-u_1, 0) = -1 < 0$, from whence the result follows. □

Theorem 5. *Under the same assumptions as Theorem 3, let $\alpha = \alpha_{\beta,1}(\varepsilon)$, $\boldsymbol{v} = (\boldsymbol{v}_x^t|\boldsymbol{v}_y^t)^t$ be a left non-zero eigenvector of J_0 associated to purely complex J_0-eigenvalue ν_1^+, and $\boldsymbol{w} = (\boldsymbol{w}_x^t|\boldsymbol{w}_y^t)^t$ be a right non-zero eigenvector of J_0 associated to $-\nu_1^+$, such that (see Theorem 1) $\boldsymbol{v}^t\boldsymbol{w} = 0$ and $\overline{\boldsymbol{v}}^t\boldsymbol{w} = 2$. Then coefficient b in Theorem 2 is given by*

$$\begin{aligned} b =& \tfrac{1}{16}\left|1-\nu_1^+ + \tfrac{\varepsilon}{\varepsilon-\nu_1^+}\right|^2 S'''(0)\cdot \\ &\cdot \operatorname{Re}\left(\left(1-\nu_1^+ + \tfrac{\varepsilon}{\varepsilon-\nu_1^+}\right)\langle \boldsymbol{v}_x, \boldsymbol{w}_x \odot \boldsymbol{w}_x \odot \overline{\boldsymbol{w}}_x\rangle\right). \end{aligned} \tag{18}$$

Proof. By Theorem 1, $\boldsymbol{v}$ can be rescaled to satisfy $\boldsymbol{v}^t\boldsymbol{w} = 0$, $\overline{\boldsymbol{v}}^t\boldsymbol{w} = 2$ which, by virtue of Equations (7) and (8), translate to

$$\left(1 - \tfrac{\varepsilon}{\varepsilon^2+|\nu_1^+|^2}\right)\boldsymbol{v}_x^t\boldsymbol{w}_x = 0, \quad \left(1 - \tfrac{\varepsilon}{(\varepsilon-\nu_1^+)^2}\right)\overline{\boldsymbol{v}}_x^t\boldsymbol{w}_x = 2, \tag{24}$$

Determining b requires knowing the first three directional derivatives of vector field $\boldsymbol{f}$. Given any direction $\boldsymbol{r} = (\boldsymbol{r}_x^t|\boldsymbol{r}_y^t)^t$, the first one is given by

$$\begin{aligned} &\sum_{k=1}^N \left(\frac{-\delta_{jk} + B_{jk}^\alpha S'\left(\sum_{l=1}^N B_{jl}^\alpha x_l\right)}{\varepsilon\delta_{jk}}\right)_{(\mathbf{0}_N,\mathbf{0}_N),0}^{l\in\{1,\dots,N\}} (\boldsymbol{r}_x)_k + \sum_{k=1}^N \left(\frac{-\delta_{jk}}{-\varepsilon\delta_{jk}}\right)_{(\mathbf{0}_N,\mathbf{0}_N),0}^{j\in\{1,\dots,N\}} (\boldsymbol{r}_y)_j \\ &= \sum_{k=1}^N \left(\frac{-\delta_{jk} + B_{jk}^0 S'(0)}{\varepsilon\boldsymbol{e}_j}\right)^{j\in\{1,\dots,N\}} (\boldsymbol{r}_x)_j + \sum_{k=1}^N \left(\frac{-\boldsymbol{e}_j}{-\varepsilon\boldsymbol{e}_j}\right)(\boldsymbol{r}_y)_j = \left(\frac{\boldsymbol{r}_x + B\boldsymbol{r}_x}{\varepsilon\boldsymbol{r}_x}\right) - \left(\frac{\boldsymbol{r}_y}{\varepsilon\boldsymbol{r}_y}\right) \\ &= \left(\frac{-\boldsymbol{r}_x - \boldsymbol{r}_y + B\boldsymbol{r}_x}{\varepsilon(\boldsymbol{r}_x - \boldsymbol{r}_y)}\right); \end{aligned}$$

now we compute the second derivative at directions $\boldsymbol{r} = (\boldsymbol{r}_x^t|\boldsymbol{r}_y^t)^t$, $\boldsymbol{s} = (\boldsymbol{s}_x^t|\boldsymbol{s}_y^t)^t$, dividing it into four terms according to the mixed partial differentiation required:

$$\begin{aligned} &\textstyle\sum_{k,m} \frac{\partial}{\partial x_m}\left(\frac{-\delta_{jk} + B_{jk}^\alpha S'\left(\sum_{l=1}^N B_{jl}^\alpha x_l\right)}{\varepsilon\delta_{jk}}\right)_{(\mathbf{0}_N,\mathbf{0}_N),0}^{j\in\{1,\dots,N\}} (\boldsymbol{r}_x)_k(\boldsymbol{s}_x)_m + \sum_{k,m} \frac{\partial}{\partial x_m}\left(\frac{-\delta_{jk}}{-\varepsilon\delta_{jk}}\right)_{(\mathbf{0}_N,\mathbf{0}_N),0}^{j\in\{1,\dots,N\}} (\boldsymbol{r}_y)_k(\boldsymbol{s}_x)_m \\ &+\textstyle\sum_{k,m} \frac{\partial}{\partial y_m}\left(\frac{-\delta_{jk} + B_{jk}^\alpha S'\left(\sum_{l=1}^N B_{jl}^\alpha x_l\right)}{\varepsilon\delta_{jk}}\right)_{(\mathbf{0}_N,\mathbf{0}_N),0}^{j\in\{1,\dots,N\}} (\boldsymbol{r}_x)_k(\boldsymbol{s}_y)_m + \sum_{k,m} \frac{\partial}{\partial y_m}\left(\frac{-\delta_{jk}}{-\varepsilon\delta_{jk}}\right)_{(\mathbf{0}_N,\mathbf{0}_N),0}^{j\in\{1,\dots,N\}} (\boldsymbol{w}_y)_k(\boldsymbol{s}_y)_m \\ &= \sum_{k,m}\left(\frac{B_{jk}^\alpha B_{jm}^0 S''(0)}{\mathbf{0}_N}\right)^{j\in\{1,\dots,N\}} (\boldsymbol{r}_x)_k(\boldsymbol{s}_x)_m + \mathbf{0}_{2N} = \sum_{k,m}\left(\frac{\mathbf{0}_N}{\mathbf{0}_N}\right) = \mathbf{0}_{2N}. \end{aligned}$$

Finally, we compute the third derivative at directions $\boldsymbol{r} = (\boldsymbol{r}_x^t|\boldsymbol{r}_y^t)^t$, $\boldsymbol{s} = (\boldsymbol{s}_x^t|\boldsymbol{s}_y^t)^t$, $\boldsymbol{t} = (\boldsymbol{t}_x^t|\boldsymbol{t}_t^t)^t$, which consists of eight terms in a similar manner of how we have previously proceeded. However, as seen is the second derivative calculations, any mixed differentiation of the form

$$\frac{\partial^2 \boldsymbol{f}}{\partial x_k \partial y_m},$$

as well as high order y_j-derivatives are all equal to zero. By means of Clairaut's theorem, we are therefore only required to compute the mixed x_j term, which reduces to

$$\begin{aligned} &\sum_{k,m,n} \tfrac{\partial}{\partial x_n}\left(\frac{B_{jk}^\alpha B_{jm}^\alpha S''\left(\sum_{l=1}^N B_{jl}^\alpha x_l\right)}{0}\right)_{(\mathbf{0}_N,\mathbf{0}_N),0}^{j\in\{1,\dots,N\}} (\boldsymbol{r}_x)_k(\boldsymbol{s}_x)_m(\boldsymbol{t}_x)_n \\ &= \sum_{k,m,n}\left(\frac{B_{jk}B_{jm}B_{jn}S'''(0)}{0}\right)^{j\in\{1,\dots,N\}} (\boldsymbol{r}_x)_k(\boldsymbol{s}_x)_m(\boldsymbol{t}_x)_n = S'''(0)\left(\frac{B\boldsymbol{r}_x \odot B\boldsymbol{s}_x \odot B\boldsymbol{t}_x}{\mathbf{0}_N}\right). \end{aligned}$$

Recall that the definition for coefficient b requires us to evaluate at eigenvalues $\boldsymbol{r} = \boldsymbol{s} = \boldsymbol{w}$ and $\boldsymbol{t} = \overline{\boldsymbol{w}}$. By remembering equivalence (6) and the fact that $B = \alpha_{\beta,1}(\varepsilon)I_N + \beta A$, we observe that

$$B\boldsymbol{w}_x = \alpha_{\beta,1}(\varepsilon)\boldsymbol{w}_x + \beta A\boldsymbol{w}_x = \alpha_{\beta,1}(\varepsilon)\boldsymbol{w}_x + (1 - \alpha_{\beta,1}(\varepsilon) - \nu_1^+ + \tfrac{\varepsilon}{\varepsilon-\nu_1^+})\boldsymbol{w}_x = (1 - \nu_1^+ + \tfrac{\varepsilon}{\varepsilon-\nu_1^+})\boldsymbol{w}_x,$$
$$B\overline{\boldsymbol{w}}_x = \alpha_{\beta,1}(\varepsilon)\overline{\boldsymbol{w}}_x + \beta A\overline{\boldsymbol{w}}_x = \alpha_{\beta,1}(\varepsilon)\overline{\boldsymbol{w}}_x + \overline{(1 - \alpha_{\beta,1}(\varepsilon) - \nu_1^+ + \tfrac{\varepsilon}{\varepsilon-\nu_1^+})}\overline{\boldsymbol{w}}_x = \overline{(1 - \nu_1^+ + \tfrac{\varepsilon}{\varepsilon-\nu_1^+})}\overline{\boldsymbol{w}}_x,$$

and therefore,

$$\left(\frac{B\boldsymbol{w}_x \odot B\boldsymbol{w}_x \odot B\overline{\boldsymbol{w}}_x}{\boldsymbol{0}_N}\right) = (1 - i\,|\lambda| + \tfrac{\varepsilon}{\varepsilon-i|\lambda|})\left|1 - i\,|\lambda| + \tfrac{\varepsilon}{\varepsilon-i|\lambda|}\right|^2 \left(\frac{\boldsymbol{w}_x \odot \boldsymbol{w}_x \odot \overline{\boldsymbol{w}}_x}{\boldsymbol{0}_N}\right).$$

We then substitute the expression for the third directional derivative in the definition for coefficient b. We obtain

$$\begin{aligned} b &= \tfrac{1}{16}\mathrm{Re}\left(\left\langle (\boldsymbol{v}_x^t|\boldsymbol{v}_y^t)^t, (1 - \nu_1^+ + \tfrac{\varepsilon}{\varepsilon-\nu_1^+})\left|1 - \nu_1^+ + \tfrac{\varepsilon}{\varepsilon-\nu_1^+}\right|^2 S'''(0)((\boldsymbol{w}_x \odot \boldsymbol{w}_x \odot \overline{\boldsymbol{w}}_x)^t|\boldsymbol{0}_N^t)^t \right\rangle\right) \\ &= \tfrac{1}{16}\left|1 - \nu_1^+ + \tfrac{\varepsilon}{\varepsilon-\nu_1^+}\right|^2 S'''(0)\mathrm{Re}\left(\left(1 - \nu_1^+ + \tfrac{\varepsilon}{\varepsilon-\nu_1^+}\right)\langle \boldsymbol{v}_x, \boldsymbol{w}_x \odot \boldsymbol{w}_x \odot \overline{\boldsymbol{w}}_x\rangle + 0\right), \end{aligned}$$

which concludes the proof. □

Corollary 1. *If matrix A is such that its strictly leading right eigenvectors are modulus-homogeneous, and $\varepsilon > 0$ is small enough, then $b < 0$ and the Hopf bifurcation undergone by system* (1) *as proved in Theorems 3 and 4 is supercritical.*

Proof. We can rescale vector $\boldsymbol{w}_x$ so that $|(\boldsymbol{w}_x)_j| = 1$ for every $j \in \{1, \dots, N\}$. This reduces formula (18) to

$$\begin{aligned} b &= \tfrac{1}{16}\left|1 - \nu_1^+ + \tfrac{\varepsilon}{\varepsilon-\nu_1^+}\right|^2 S'''(0)\sum_{j=1}^N \mathrm{Re}\left((1 - \nu_1^+ + \tfrac{\varepsilon}{\varepsilon-\nu_1^+})(\overline{\boldsymbol{v}}_x)_j(\boldsymbol{w}_x)_j\,|(\boldsymbol{w}_x)_j|^2\right) \\ &= \frac{1}{16}\left|1 - \nu_1^+ + \frac{\varepsilon}{\varepsilon - \nu_1^+}\right|^2 S'''(0)\sum_{j=1}^N \mathrm{Re}\left(\left(1 - \nu_1^+ + \frac{\varepsilon}{\varepsilon - \nu_1^+}\right)(\overline{\boldsymbol{v}}_x)_j(\boldsymbol{w}_x)_j\right) \\ &= \frac{1}{16}\left|1 - \nu_1^+ + \frac{\varepsilon}{\varepsilon - \nu_1^+}\right|^2 S'''(0)\mathrm{Re}\left(\left(1 - \nu_1^+ + \frac{\varepsilon}{\varepsilon - \nu_1^+}\right)\overline{\boldsymbol{v}}_x^t\boldsymbol{w}_x\right) \\ &= \frac{1}{8}\left|1 - i\,|\lambda| + \frac{\varepsilon}{\varepsilon - \nu_1^+}\right|^2 S'''(0)\mathrm{Re}\left(\left(1 - \nu_1^+ + \frac{\varepsilon}{\varepsilon - \nu_1^+}\right)\left(\frac{(\varepsilon - \nu_1^+)^2}{(\varepsilon - \nu_1^+)^2 - \varepsilon}\right)\right). \end{aligned}$$

As locally odd sigmoid function S is assumed to satisfy $S'''(0) < 0$ (see Subsection II-A), it is clear that the sign of coefficient b is opposite to that of the real-part term in the previous expression, whose argument z is given by

$$z = \left(1 - \nu_1^+ + \frac{\varepsilon}{\varepsilon - \nu_1^+}\right)\left(\frac{(\varepsilon - \nu_1^+)^2}{(\varepsilon - \nu_1^+)^2 - \varepsilon}\right). \quad (25)$$

To determine the sign of $\mathrm{Re}(z)$ we need to substitute the values for $\left|\nu_1^+\right|$, as before, by splitting the proof into a real and non-real case. Recall that in the real case we get the expression $\left|\nu_1^+\right| = \sqrt{\varepsilon(1-\varepsilon)}$ from Equation (11). Then

$$z = (1+\varepsilon)\frac{\varepsilon - \frac{1}{2} - i\sqrt{\varepsilon(1-\varepsilon)}}{\varepsilon - 1 - i\sqrt{\varepsilon(1-\varepsilon)}} = (1+\varepsilon)\frac{\frac{1}{2}(1-\varepsilon) - \frac{3}{2}i\sqrt{\varepsilon(1-\varepsilon)}}{(1-\varepsilon)^2 + \varepsilon(1-\varepsilon)},$$

and thus $\mathrm{Re}(z) > 0$ for $\varepsilon \in (0,1)$, therefore $b < 0$. For the non-real case we directly evaluate at the singular limit,

$$\begin{aligned} &\lim_{\varepsilon\to 0^+}\mathrm{Re}\left(\left(1 - i\,|\lambda| + \frac{\varepsilon}{\varepsilon - i\,|\lambda|}\right)\left(\frac{(\varepsilon - i\,|\lambda|)^2}{(\varepsilon - i\,|\lambda|)^2 - \varepsilon}\right)\right) = \mathrm{Re}\left(\left(1 - iv + \frac{0}{0 - iv}\right)\left(\frac{(0 - iv)^2}{(0 - iv)^2 - 0}\right)\right) \\ &=\mathrm{Re}\left((1 - iv)\left(\frac{-v^2}{-v^2}\right)\right) = \mathrm{Re}(1 - iv) = 1 > 0. \end{aligned}$$

This concludes that term z from (25) has positive real part, thus proving that b is negative for small enough values of $\varepsilon > 0$, therefore making the bifurcation supercritical, which is what we wanted to prove. □